جمهوريه العراق
وزاره التعليم العالي والبحث العلمي
كليه العلوم للبنات

تصنيع المتراكب النانوي (شيتوزان /أوكسيد التيتانيوم / فضه) بواسطه القشط الليزري للتطبيقات البيئية

رساله

مقدمه الى مجلس كليه العلوم للبنات/جامعه بابل ضمن متطلبات الحصول على

درجه الماجستير في فيزياء الليزر

من قبل

تبارك عبد زيد الطائي
بكالوريوس (2019)

بأشراف

أ.م.د امير خضير النافعي

أ.م جنان علي عبد

1445 هجري

2023 ميلادي

Republic of Iraq
Ministry of Higher Education and Scientific Research
University of Babylon
College of Sciences for Women
Department of Laser Physics

Synthesis of Chitosan/TiO_2/Ag Nanocomposite by Pulsed Laser Ablation for Environmental Applications

A Thesis

Submitted to council of the College of Sciences for Women /University of Babylon as part of the requirements for obtaining a master's degree in laser physics

By

Tebark Abd Zaid Al-Taie

B.Sc. (2019)

Supervised by

Asst. Prof. Dr. Amer Khudair Al-Nafiey

Prof. Dr. Jinan Ali Abd

2023 1445

بسم الله الرحمن الرحيم

يَرْفَعِ اللَّهُ الَّذِينَ آمَنُوا مِنْكُمْ وَالَّذِينَ أُوتُوا الْعِلْمَ دَرَجَاتٍ وَاللَّهُ بِمَا تَعْمَلُونَ خَبِيرٌ

صدق الله العلي العظيم

سورة المجادلة، آية: (11)

Dedication

To the Lady of the Two Universes, the river of knowledge, the source of chastity, and the crown of modesty, my Lady Fatima Al-Zahra, peace be upon her.

To the one who filled the earth with fairness and justice after it was filled with oppression and oppression, the owner of the family of Muhammad.

To the one who enlightened my path, my pillar, and my refuge.

whose prayers accompany my steps,

my father.

To the one who sprouts in her heart the flowers of love.

To whom heaven is under her feet.

To the eye where I saw safety,

My beloved mother.

To the backbone that I lean on in difficult times.

To the bright stars in my sky,

My brothers.

To my soul sanctuary and travel companion.

To the partner of my dreams who walked with me to make them come true,

My husband.

I dedicate the fruit of my humble effort.

Tebark Al- Taie

Acknowledgments

Praise be to God, Lord of the worlds, and praise be to God always abundant, never cease and prayers and peace be upon our prophet Muhammad and his family. I extend my thanks and great appreciation and respect to the professors who supervised the research **(Dr. Amer Khudhair Al-Nafiey)** and **(Dr. Jinan Ali Abd)** for all the moral and scientific assistance they provided me with in completing this work.

I extend my thanks and appreciation to my family and my husband's family for their support during the study period.

I extend my thanks and appreciation to the Department of Laser Physics with all its affiliates, especially the Deanship of the College of Sciences for Women for their support during the study period.

Last but not least, thanks and appreciation to all my professors in all stages of my academic life, thanks to all my colleagues, and may God grant them success in their scientific lives.

Tebark

LIST OF CONTENTS

TABLE LIST

FIGURE LIST

List of Symbols &Shapes

Symbols	Meaning
α	Absorption Coefficient
A	Absorbance
Ag	Silver
CS	Chitosan
C.S	Crystallite Size
DNA	Dioxy Nucleic Acid
Eg	Energy Gap
EDX	Electron energy dispersive technology
E.coli	Escherichia coli
FWHM	Full Width at Half Maximum
FTIR	Fourier transform infrared spectroscopy
I	Transmitted Photon Intensity
I_0	Incident Photon Intensity
K.	Klebsiella
NP_S	Nanoparticles
θ	Bragg's Angle
PLAL	pulsed laser ablation in liquid
ROS	Reactive Oxygen Species
SEM	Scanning Electron Microscopy
TEM	Transmission Electron Microscope
TiO_2	Titanium Dioxide
UV	Ultra Violet Wavelength

UV-Vis	Ultraviolet-visible UV -Vis diffuse reflectance
XRD	X- ray Diffraction
λ	Wavelength

Examination Committee Certification

We certify that after reading this thesis, entitled:**" Synthesis of Chitosan/TiO_2/Ag Nanocomposite by Pulsed Laser Ablation for Environmental Applications"** , and as committee, examined the student **"Tebark Abd Zaid Al-Taie"** its contents and that in our opinion it meets the standards of a thesis for the Degree of Master of Science in Laser Physics and its Application.

Signature:
Name: **Dr. Alaa Jewad Kadhem Algidsawi**
Title: Professor
Date: / / 2023
(Chairman)

Signature:
Name: **Dr. Saddam Flayeh Haddawi**
Title: Assistant Professor
Date: / / 2023
(Member)

Signature:
Name: **Dr. Hamsa Naji Naser**
Title: Assistant
Date: / / 2023
(Member)

Signature:
Name: **: Dr. Amer Khudair Al-Nafiey**
Title: Assistant Professor
Date: / /2023
(Member/Supervisor)

Signature:
Name: **: Dr. Jinan Ali Abd**
Title: Professor
Date: / / 2023
(Member/Supervisor)

Approved by the Dean of College
Signature:
Name: **Dr. Abeer Fawzi Al-Rubaie**
Title: Professor
Address: Dean of the College of Science for Women.
Date: / / 2023

Supervisor certificate

We certify that this thesis entitled **"Chitosan/TiO2/Ag Nanoparticles: Synthesis And Characterization By Pulsed Laser Ablation For Environmental Application "** was prepared by the student **(Tebark Abd Zaid)** under our supervision at the department of Laser physics, College of Science for Women, University of Babylon, as a partial fulfillment of the requirements of the degree of Doctorate of philosophy in laser physics and its applications.

Signature by

Asst. Prof. Dr. Amer Khudair Al-Nafiey prof. Dr. Jinan Ali Abd

Date: / / 2021

Head of the Department Certificate

In view of the available recommendations, I forward this dissertation for debate by the examining committee.

Signature:
Name: ***Jinan Ali Abd***
Title: **Prof. Dr.**
(Head of Laser Physics Department)
Date: / /2021

الخلاصة

في هذه الدراسة تم تحضير المركبات النانوية [شيتوزان-أكسيد التيتانيوم-الفضة [(CS-TiO_2-Ag)، شيتوزان-أكسيد التيتانيوم (CS-TiO_2)، شيتوزان-الفضة (CS-Ag)] عن طريق الاستئصال بالليزر النبضي في السوائل باستخدام ليزرND:YAG كان الطول الموجي 1064 نانومتر، التردد 1 هرتز، الطاقة 500ml، مع عدد نبضات مختلف للمواد النانوية كانت نبضة (1000)CS-TiO_2 ونبضة (500)CS-Ag.

أظهرت نتائج الامتصاص للمواد قمه مميزة لامتصاص الشيتوزان- الفضة عند 400nm، وامتصاص الحافة لأكسيد الشيتوزان- تيتانيوم عند 375nm، وامتصاص الحافة للشيتوزان عند 275nm.

بينما تكون فجوة الطاقة في المركبات النانوية {((Ag، (TiO_2)، (CS)، (CS-Ag)، (CS-TiO_2)، (CS TiO_2-Ag} [1.6, 2.5, 2.9, 2.37, 2.38, 2.1]eV علي التوالي.

ومن خلال نتائج مطياف فورييه لتحويل الأشعة تحت الحمراء [FTIR] ظهرت روابط كيميائية بين المواد النانوية (أكسيد الفضة والتيتانيوم) مع البوليمر.

أظهر تحليل حيود XRD أن TiO_2 وAg كانا متبلورين وأن متوسط أحجام البلورات لـ CS-Ag، و-CS TiO_2، وCS-TiO_2-Ag كانت (5.95,5.96,5.96)nmعلى التوالي.

علاوة على ذلك، أظهرت صور SEM الشكل شبه كروي، ويبلغ متوسط حجم حبيبات الجسيمات النانوية 95nm. كما تم توصيفها باستخدام فحص TEM الذي أظهر أحجام نانوية مختلفة لـ CS(13)nm ، CS-TiO_2 (15)nm ، CS-Ag (34)nm ، و CS-TiO_2-Ag (32)nm.

تم تطبيق المركبات النانوية كعوامل مضادة للجراثيم لقتل بكتيريا E.coli وتثبيط بكتيريا Klebsiella. تم قياس مناطق القتل للإشريكية القولونية على النحو التالي: CS (20)mm ، CS-Ag (36)mm ، CS-TiO_2 (38)mm ، وCS-TiO_2-Ag (40)mm. بينما تم قياس تثبيط بكتيريا الكلبسيلا كما يلي: CS (28)mm ، CS-Ag (35)mm ، CS-TiO_2 (38)mm ، وCS-TiO_2-Ag (43)mm.

وأخيراً تمت دراسة التطبيق البيئي لـ CS-TiO_2-Ag في تنقية المياه. تم ترشيح 30ml من الماء الملوث من خلال المرشح الذي تم تصنيعه، ثم تمت إضافة 30ml من مركب النانو (CS-TiO_2-Ag) لمدة 10min وتم حساب تغيرات الامتصاص. وكانت النتيجة كفاءة تنقية المياه بنسبة 50%.

Abstract

In the current study, nanocomposites [Chitosan-Titanium Oxide-Silver (CS-TiO_2-Ag), Chitosan-Titanium Oxide (CS-TiO_2), Chitosan-Silver (CS-Ag)] were prepared by pulsed laser ablation in liquids. ND:YAG laser was used with a 1064 nm wavelength, 1 Hz frequency, 500 mJ energy with different pulse numbers of the nanocomposites of CS-TiO_2(1000) pulse and CS-Ag(500) pulse.

The absorption results of the materials showed characteristic peaks absorption for Chitosan- silver at 400 nm, edge absorption Chitosan- titanium oxide at 375 nm and edge absorption chitosan at 235 nm.

While the energy gap of {(Ag), (TiO_2), (CS), (CS-Ag), (CS-TiO_2), (CS-TiO_2-Ag)} nanocomposites were found to be [1.6, 2.5, 2.9, 2.37, 2.38, 2.1] eV, respectively.

Through the results, Fourier Transform Infrared Spectrometer [FTIR], chemical bonds appeared between the nanomaterials (silver and titanium oxide) with the polymer.

The XRD diffraction analysis revealed that TiO_2 and Ag were crystalline and the average crystal sizes for CS-Ag, CS-TiO_2, and CS-TiO_2-Ag were 5.96, 5.96, and 5.95 nm, respectively.

Moreover, the SEM images showed the shape as semi- spherical, and the average grain size of the nanoparticles is 95 nm. Also the were characterized using TEM examination, which revealed different nanosizes of CS (13) nm, CS-TiO_2 (15 nm), CS-Ag (34) nm, and CS-TiO_2-Ag (32) nm.

The nanocomposites were applied as antibacterial agents to kill *E.coli* bacteria and inhibit *Klebsiella* bacteria. The killing areas for *E.coli* were measured as follows: CS (20 mm), CS-Ag (36 mm), CS-TiO_2 (38 mm), and CS-TiO_2-Ag (40 mm). While for inhibit *Klebsiella* bacteria, they were measured as follows: CS (28 mm), CS-Ag (35 mm), CS-TiO_2 (38 mm), and CS-TiO_2-Ag (43 mm).

Finally, the environmental application of CS-TiO_2-Ag in water purification was studied. A 30 ml of polluted water was filtered through the filter that was

manufactured, and then a 30 ml of the nanocomposite (CS-TiO_2-Ag) was added for 10 minutes and the absorbance changes were calculated. Results showed a water purification efficiency of 50%.

Chapter one

General Introduction and previous studies

Chapter Two

The Theoretical Part

Chapter Three

Experimental Work

Chapter Four

Results and Conclusion

1.1 Introduction

Nanotechnology has undergone significant advancements in recent decades, offering a new tool for innovation and progress across various fields. It is a distinguishing characteristic is its tiny size, which reaches the nanometer scale. These nanomaterials have found numerous applications in various domains, including medicine, industry, electronics, and environment. It is also demonstrating a remarkable efficacy in combatting bacteria and purifying water. Examples of such materials encompass zinc, copper, gold, silver, titanium, as well as certain types of polymers and oxides such as silver oxide, titanium oxide, zinc oxide, nano carbon, silicon oxide, and more [1].

Polymer nanocomposites offer significant potential in the development of advanced materials for numerous applications. These novel materials benefit from the synergy between filler particles and polymer chains that are on similar length scales and the large quantity of interfacial area relative to the volume of the material [2]. Examples of polymers are (Poly (lactic-co-glycolic acid)) PLGA Nanoparticles [3], Polyethylene oxide (PEO) Nanocomposites [4], Poly (methyl methacrylate) (PMMA) Nanocomposites [5] and chitosan [6].

The preparation of nanomaterials needs various methods. Chemical methods include Sol-gel treatment for stability [7], chemical precipitation [8], and chemical vapor deposition [9]. Physical methods encompass vapor condensation [10], thermal spraying [11], laser melting [12], and pulsed laser ablation [13].

In the same context, a nanocomposite (CS-TiO_2-Ag) was prepared via pulsed laser ablation in liquids and its properties, as well as its medical and environmental applications wear studied.

1.2 Nanomaterials

Nanomaterials' dimensions are ranging from 1-100 nanometers. They are classified according to the shape and size of the particles to several categories such as nanoparticles, nanocrystals, nanotubes, nanofibers, and nanosheets. The properties of these nanomaterials vary based on their size, shape, and chemical composition [14].

The properties of these materials are unique and not found in bulk materials. Among these unique properties are electromechanical, optical, chemical, and thermal properties. These properties make nanomaterials interesting in a variety of scientific and technical applications [15].

Nanomaterials are classified according to their dimensions into dimensionless nanomaterials: zero-dimensional nanomaterials: these nanomaterials have three dimensions at the nanoscale, and include nanoparticles, such as nanospheres, quantum dots, and metallic nanoparticles [16].One-Dimensional Nanomaterials: these that have one dimension at the nanoscale. They include nanotubes, fibers, wires, carbon nanofibers and quantum wires [17]. Two-Dimensional Nanomaterials: these, which have two dimensions at the nanoscale. They include graphene sheets, nanosheets, and membranes [18].

1.3 Manufacturing of Nanomaterials

There are many available methods for manufacturing nanomaterials but generally two basic approaches: the top-down approach and the bottom-up approach.

1-**Top-down approach**: In this approach, larger materials are broken into smaller pieces. This can include technologies such as mechanical milling, laser engraving, and chemical finishing…..etc. [19].

2- Bottom-up approach: In this approach, nanomaterials are built from atoms and molecules. These methods can include self-assembly, surface chemistry, and chemical vapor deposition. Therefore, this approach can produce uniformly sized, structured parts; however, it may require certain conditions or advanced equipment's [20].

In both methods, the final properties of the nanomaterial can be modified by controlling the chemical and physical processes involved in its synthesis. Size, shape, composition, and structure, including surface properties, can be controlled to produce nanomaterials with specific properties. These properties can make nanomaterials useful in a wide range of applications, such as electronics, medicine, energy, environment, and ultra-strong materials [17].

1.4 Methods for Manufacturing Nanomaterials

There are two ways to prepare nanomaterials, the chemical method and the physical method , each of them includes several methods:

a. Chemical methods include thermal decomposition, Chemical Vapor Deposition CVD, Self-assembly, Chemical Bath Deposition CBD, Hydrothermal method [21-25].

b. Physical methods include Physical Vapor Deposition (PVD) [26], Ball Milling [27], Pulsed Laser Deposition (PLD) [28], Organic Metal Vapor Phase Epitaxy (OMVPE) [29], and Pulsed Laser Ablation in Liquids PLAL [30, 31].

Each one differs from the other, having advantages and disadvantages. However, in this work, the method of pulsed laser ablation in liquids is used as an easy and safe physical method. It is used to obtain nanomaterials in small.

1.5 Pulsed Laser Ablation in Liquids (PLAL)

It is one of the techniques used to fabricate nanoparticles from various materials. The process begins by directing a powerful laser pulse at a solid target immersed in a liquid. When the laser pulse reaches the target, it interacts with the surface and generates high energy producing plasma. This plasma consists of atoms, ions and electrons of the target substance. Some of the material is separated from the target and turns into vapor. This vapor expands in the surrounding liquid forming a bubble that contains the plasma [32].

Over the time, the bubble cools and contracts, allowing atoms and ions in the plasma to come together and form nanoparticles. The properties of the resulting nanoparticles can be controlled by controlling the operation conditions, such as laser power, duration, and laser wavelength, in addition to the type of liquid used and the type of target material as shown in figure (1-1) which illustrates the ablation process. This method offers several advantages it allows obtaining nanoparticles of uniform size and free of impurities, which can be used to generate nanomaterials with a wide variety of materials and compositions. Additionally, this process is environmentally friendly since no harmful chemicals are used [33, 34].

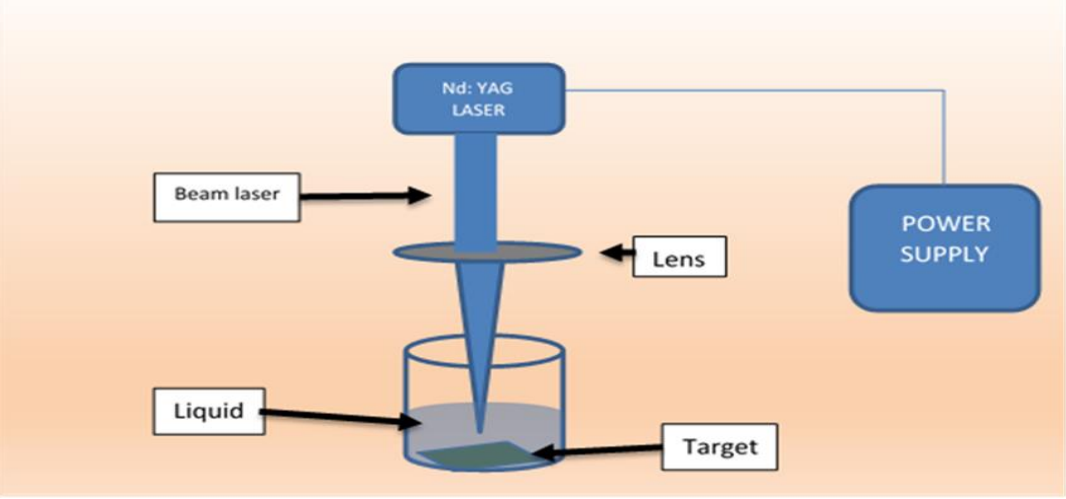

Figure (1-1): Describes the pulsed laser ablation of liquid

1.6 Utilized Materials in This Study

1.6.1 Chitosan

Chitosan is a natural compound consisting of glucosamine units that are linked by beta 1-4 glycosidic bonds. Glucosamine is a glucose molecule that has been modified so that it contains an amine group (NH_2) instead of a hydroxyl group (OH) As in Figure (1-2). Its structure depends on the production method [35] and is derived from chitin found in the cell walls of plants, the shells of mollusks, and the hard shells of ticks and insects. Chitosan has several properties such as water solubility, low toxicity, and the ability to form films and gel structures. Because of these properties, chitosan is used in a wide range of applications in areas such as energy, environment, wastewater purification, and as an antimicrobial agent [36].

It is also used in agriculture, as chitosan is considered a plant growth stimulant and a health enhancer. It can improve soil quality and increase plant resistance to diseases and pests [37]. Moreover, chitosan can be used to improve food quality and shelf life [38, 39]. In the environmental field, chitosan can be used as an adsorbent to remove contaminants making it an ideal candidate for the biological removal of heavy metals, dyes and organic compounds in aquatic systems. Chitosan has high efficacy against a variety of bacteria, including *Escherichia coli and Klebsiella* [40]. It is believed that the mechanism of action of chitosan as an antimicrobial agent is related to the electrical interactions between positive chitosan and negative bacteria, which leads to deformation of the bacterial cell wall and leakage of proteins and nuclear materials thus killing the bacteria [41, 42].

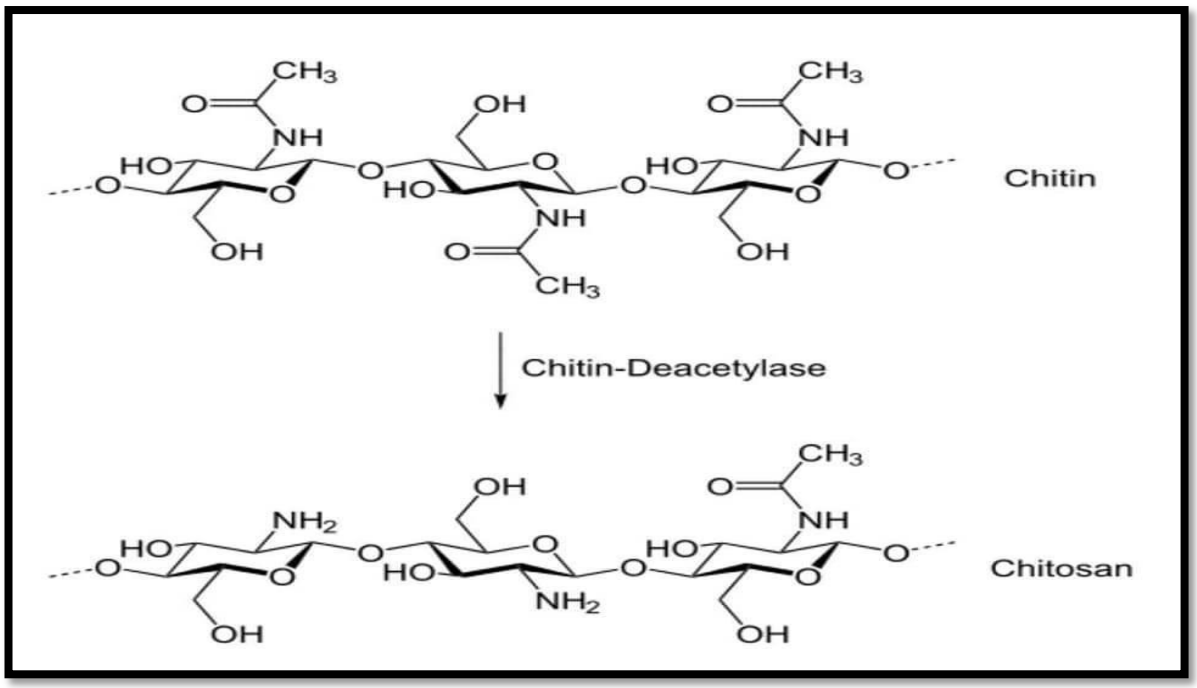

Figure (1-2): Formation of chitosan by partial deacetylation of chitin [35].

Table (1-1): Explains the properties of chitosan

Property	Description	Ref.
Chemical Structure	Organic polymer derived from chitin	[6]
Color	Colorless	[43]
Solubility	soluble in water	[43]
Melting Point	Varies with degree of deacetylation	[44]
Biodegradability	Natural material and biodegradable by biological enzymes	[6]
Insulating Ability	Chitosan materials typically do not have an energy gap due to their organic nature	[45]

This table summarizes the properties of chitosan and indicates the absence of an energy gap due to its organic nature.

1.6.2 Titanium Dioxide (TiO_2)

Titanium Dioxide (TiO_2) is a chemical compound consisting of two elements, titanium and oxygen. This compound is characterized by its distinct physical and chemical properties, making it a valuable material in a wide range of applications [46].Prominent features include its chemical stability, the ability to withstand high temperatures, and resistance to corrosion [47]. In terms of energy gap, titanium dioxide has a wide energy gap ranging from 3.0 to 3.2 electron volts [48]. However, when exposed to light, reactions occur in the upper layers of titanium oxide that can produce free electrons, and thus it is able to conduct electricity with high efficiency. This property makes it an ideal material for using in many photovoltaic applications, including solar cells and photocatalysts [49]. One of the main characteristics of nanoscale titanium oxide is its large surface area compared to volume, which makes it ideal for use in applications that require surface reaction, such as catalysts [50]. One of the important applications of titanium dioxide is its ability to kill bacteria and viruses. Titanium dioxide is a catalyst present in many products used to disinfect water, air, and surfaces [51]. This material is characterized by its ability to generate free radicals and reactive oxygen when exposed to light, which allows it to effectively kill bacteria and viruses [52].

Table (1-2): The chemical and physical properties of titanium dioxide

Properties	Description	Ref.
Atomic Mass	79.866 atomic mass units (am u)	[53]
Color	Colorless in pure form, may exhibit various colors	[53]
Melting Point	Approximately 1843 degrees Celsius	[53]

Hardness	High and solid, making it resistant to corrosion and impacts	[54]
Thermal Insulation	Poor heat conduction, acts as a thermal insulator	[46]
Chemical Stability	Chemically stable and non-reactive with most chemicals	[46]
Light Reflectivity	High light-reflecting ability	[54]

1.6.3 Sliver (Ag)

Silver (Ag) is a precious metal with many unique properties and multiple applications. Silver has been used since ancient times in money, jewelry, eating utensils, and many other purposes because of its unique physical and chemical properties [55]. Silver is one of the best conductors of electricity and heat, which makes it an important component in many electrical and electronic applications. It is also characterized by its durability, formability, and flexibility, which facilitate its use in a wide range of applications [56].

However, is the use of silver as an antibacterial. Scientists discovered that silver is able to kill and prevent the reproduction of bacteria and other microbes, has the ability this discovery led to multiple applications in the medical and health fields, including protective clothing, adhesives, and medical devices [57]. With regard to properties Electrical properties of silver, it has a high quality of electrical conductivity. This is due to the low energy gap in silver, which is the gap between the upper occupied level of electrons and the lower unoccupied level. Because of this small gap, electrons can easily transfer between levels, making silver an excellent conductor of electricity [58].

Table (1-3): Physical and Chemical Properties of Silver

Property	Value	Ref.
Atomic Number	47	[59]
Atomic Mass	107.87 g/mol	[60]
Density	10.49 g/cm³	[61]
Melting Point	961.8 °C	[62]
Boiling Point	2162 °C	[63]
Color	Silver	[64]
Electrical Conductivity	Excellent	[65]
Thermal Conductivity	Excellent	[66]
Luster	High	[67]
Hardness	2.5 (on the Mohs scale)	[68]
Malleability and Ductility	Excellent	[65]
Optical Transparency	Excellent	[65]
Chemical Reactivity	Low reactivity with oxygen, sulfur, and some chemical compounds.	[69]
Common Applications	Used in coins, jewelry, silverware, mirrors, glass lenses,electronics, medical devices, and various industrial applications.	**[70]**

1.7 Nanomaterials as Antibiotics

Nanomaterials have shown a potential antibiotic efficacy, due to their unique properties associated with nanoscale dimensions. In general, nanoparticles have a significantly increased surface area compared to their size, meaning that they can provide more interactive chemical interfaces [71, 72] .In the context of antibiotics, nanoparticles could improve permeability and targeting that enables then reach places where large particles cannot reach. In addition, nanoparticles can used deliver antibiotics directly to target sites, reducing the doses required and potential side effects [73].The proper example is silver nanoparticles that exhibit antibacterial properties, as they can destroy bacteria by penetrating into the cell membrane and interacting with proteins and DNA within the cell. [74]. Titanium oxide nanoparticles (TiO_2 NPs) are effective antibiotics, as they can stimulate the formation of free radicals under the influence of light, which leads to damage to bacterial cells [75], which is the same behavior of gold nanoparticles [76] and nanotubes of zinc oxide [77,78] .

1.8 Bacteria (forms, characteristics, and types)

Bacteria exhibit considerable diversity in their shapes. Bacteria can be spherical (known as cocci), rod-shaped (bacilli), spiral-shaped (spirochetes), or even pleomorphic, meaning that they can take on several different shapes [79] .Bacterial cellular structure is another defining characteristic, bacteria are typically classified as either gram-positive or gram-negative. This is determined by the structure of the cell wall. Gram-positive bacteria have a thicker cell wall, whereas gram-negative bacteria have a more complex and thinner cell wall [80]. Bacteria's habitat and method of

acquiring nutrition also vary. Some bacteria live in environments devoid of oxygen termed anaerobic, while aerobic bacteria require oxygen .

Additionally, there are chemotrophic bacteria, which derive their energy from chemical reactions, and phototrophic bacteria, which use light as an energy source [81]. Examples of known bacterial species include Escherichia coli, Klebsiella, Staphylococcus aurous, Streptococcus pyogenic, Clostridium botulinum, Bacillus anthracis, among many others. Each type has specific characteristics and a range of environments that they can survive in [82]. Some bacterial species can cause diseases in humans, animals, and plants. For instance, Salmonella and E. coli can cause gastrointestinal disturbances, while Gonorrhea can cause inflammations in humans [83].

Beneficial bacteria also exist and play crucial roles in a multitude of biological and environmental processes. For example, the bacteria in our intestines aid in food digestion and vitamin production, while those in the soil contribute to the nitrogen cycle and organic matter decomposition [84].

1.9 Escherichia coli

Escherichia coli, commonly known as *E. coli*, is a type of bacteria that lives in the intestines of healthy humans and animals. Most varieties of *E.coli* are harmless and actually an important part of a healthy human intestinal tract. However, some *E.coli* are pathogenic, either diarrhea or illness outside of the intestinal tract. The types of

E.coli that can cause diarrhea can be transmitted through contaminated water or food, or through contact with animals or people [85].

Escherichia coli (E.coli) is a gram-negative bacterium. This indicates the structure of the cell wall, which can be determined by the Gram test, a staining technique widely used in microbiology laboratories. Gram-negative bacteria such as *E.coli* the cell wall, consists of two main layers: a thin peptidoglycan layer, which surrounds the inner plasma membrane, and an outer layer, which contains glycoproteins and lipopolysaccharides. This outer layer confers Gram-negative bacteria resistance to a number of antibacterial drugs and host immunosuppressant. The cell wall of *E.coli* not only protects and gives shape to the cell, but also plays a role in interacting with its environment. Therefore, understanding the structure and functions of the cell wall can be useful in developing strategies to combat diseases caused by infection with bacteria [86].

1.10*Klebsiella*

Klebsiella pneumonia is a type of Gram-negative bacteria typically found in the environment and in the human intestines, where it can live without causing disease. However, K. pneumoniae can sometimes cause serious types of infections, including pneumonia (hence its name), urinary tract infections, liver abscesses, and meningitis [87] .A prominent characteristic of K. pneumoniae is its large mucous capsule, which provides protection from the body's immune system as well as from certain types of antibiotics [88]. Emerging antibiotic resistance in K. pneumoniae is a public health concern, as it is capable of developing resistance to many drugs, including carbapenems and colistin, which were previously considered "last-resort" drugs for infections unresponsive to other antibiotics [89].

1.11Bacterial killing mechanisms

1- Bacteria can be killed by oxidative damage. Reactive oxygen species (ROS), such as hydrogen peroxide, superoxide, and hydroxyl radicals, can be particularly damaging to bacteria. They can damage DNA, proteins, and lipids, leading to cell death [90].

2- The human immune system has numerous ways to kill bacteria. Phagocytes such as macrophages and neutrophils can engulf bacteria and destroy those using enzymes and antimicrobial peptides. Additionally, the immune system can produce antibodies that neutralize bacteria or mark them for destruction [77].

3- Bacteriophages are viruses that infect bacteria and can lead to bacterial cell death. After a bacteriophage infects a bacterial cell, it replicates inside the cell and then causes the cell to burst, or lyse, releasing new phage particles. This lysis kills the bacterial cell [91].

4- Antibiotics a major method of bacterial killing. These drugs typically target essential bacterial processes, such as cell wall synthesis, protein synthesis, and DNA replication. When these processes are inhibited, the bacteria cannot grow and divide, leading to cell death [92].

1.12 Literature Review

In 2014, Haldorai and et.al. Prepared and studied the antibacterial and photocatalytic properties of a new nanoscale hybrid of chitosan-titanium dioxide. The hybrid nanoparticles have been characterized by several techniques, including transmission electron microscopy and infrared spectroscopy. The results showed that the nano-hybrid possesses strong antibacterial the a of 100% within 24 h of treatment against Escherichia coli (E. coli) was measured by colony forming units (CFU) and photocatalytic properties, making it a strong candidate for environmental and medical applications. These results indicate that the hybrid chitosan-titanium dioxide nanoparticles may be effective in applications such as disinfection and decomposition of organic pollutants under sunlight [93].

In 2016, Salman prepared TiO_2 nanoparticles using a method of laser evaporation in liquid. This was achieved by directing Nd: YAG lasers with wavelengths of 532 nanometers and 1064 nanometers towards a target of titanium submerged in deionized water. The synthesized products were characterized using advanced techniques such as X-Ray Diffraction (XRD), Atomic Force Microscopy (AFM), and UV-Visible (UV-Vis) spectrophotometry. The results from this study indicated the successful synthesis of TiO_2 nanoparticles at room temperature. The average diameter of these nanoparticles was approximately 84.78 nanometers for the 1064-nanometer laser wavelength and about 95.96 nanometers for the 532-nanometer laser wavelength. Additionally, optical property studies showed that these particles exhibited a direct optical transition with energy band gaps of 3.82 electron volts for the 1064-nanometer laser wavelength and 3.65 electron volts for the 532-nanometer laser wavelength [94].

In 2016, Raut and et.al conducted experiments for the preparation and characterization of chitosan-titanium dioxide nanocomposites, and measured their antimicrobial activity under visible light. The sol–gel and ultra-sonication method assisted for the

preparation of Chitosan-TiO_2: Cu (CS-CT) nanocomposite. The structural properties of prepared CS-CT nanocomposite were studied by XRD and FTIR techniques. The XPS was used to estimate elemental composition of the nanocomposite. Thermal properties were studied using TGA. TEM and SEM analysis showed the non-spherical nature of NPs with the average mean diameter 16 nm. The optical properties were analyzed with UV–vis diffuse reflectance spectroscopy to confirm optical absorption in the visible region of light. Where CS-CT showed 200% enhanced light mediated photocatalytic antimicrobial activity against microorganism (Escherichia coli and Staphylococcus aurous) as compared with control. The results demonstrated that the nanocomposites effectively killed bacteria under the influence of visible light, suggesting potential uses in applications requiring bacterial disinfection, such as water and medical surface disinfection [95].

In 2017, Regiel-Futyra et.al. Developed non-cytotoxic silver-chitosan nanocomposites aimed to effectively controlling biofilm-forming microorganisms. Given that biofilms can lead to severe health issues and can exhibit resistance to conventional antibiotics, the need for novel solutions is paramount. The results showed high efficacy of these silver-chitosan nanocomposites in eliminating biofilm-forming microorganisms, while preserving critical safety attributes like non-toxicity to cells. This suggests these nanocomposites could serve as an effective treatment against infections triggered by biofilms [96].

In 2018, Jbeli and et.al investigated the synthesis and photocatalytic properties of chitosan-silver-titanium dioxide films. The surface of chitosan thin films was modified in heterogeneous phase via a simple and straightforward mild chemical process: chemisorption of silver ions followed by the synthesis in situ of TiO_2 at low temperature (100 °C), the using techniques like X-ray diffraction, scanning electron microscopy, and UV-visible spectroscopy. The films demonstrated outstanding

photocatalytic activity under visible light, suggesting potential applications in environmental remediation such as degradation of organic pollutants [97].

In a 2020, Menazea and Awwad this article attempt to synthesis titanium dioxide (TiO_2) doped zinc oxide (ZnO) composite via Pulsed Laser Ablation in Liquids (PLAL) and study its antibacterial properties. The structure, optical, morphological of the prepared composite have been investigated via various technique. XRD measurements approved the enhanced crystallinity ZnO after doped by TiO_2 via PLAL technique. The optical transmittance was enhanced from 78.6% of pure ZnO to 92.3% for TiO_2 doped ZnO. Moreover, the cell viability has been studied for the papered pure ZnO and TiO_2 doped ZnO. The minimum cell viability ratio was about 81.4 ± 4.2% for pure ZnO and was increased to 91.6 ± 5.1% for TiO_2 doped ZnO. The antibacterial activity of the samples that measured via MIZ approved that the TiO_2 doped ZnO make a raise in the activity index. It was suggested that TiO_2 doped ZnO can be used in many antimicrobial application [98].

In 2020, Menazea and et.al. investigated the synthesis, physical characterization, and antibacterial properties of a polyvinyl alcohol (PVA)/chitosan matrix doped with selenium nanoparticles, prepared using a one-pot laser ablation method. This technique allowed for quick, eco-friendly synthesis of nanoparticles. The material displayed significant antibacterial activity, suggesting potential applications in developing new antimicrobial materials [99].

In 2021, Khashan and et.al used a one-step laser ablation technique in liquid to explore the synthesis and antibacterial properties of TiO_2 nanoparticles. The synthesized nanoparticles exhibited significant antibacterial activity against a variety of bacterial strains, indicating potential applications in the biomedical field as an antibacterial agent [100].

In 2021, Khashan and et.al. used a laser ablation technique in liquid to explore the synthesis and antibacterial properties of TiO_2 nanoparticles The samples were characterized using UV–visible absorption spectra obtained with a UV–visible spectrophotometer (UV-Vis,) Fourier transform infrared (FTIR), X-ray diffraction (XRD), and transmission electron microscope (TEM). While, UV-Vis spectra showed the characteristic band-to-band absorption peak of TiO_2 NPs in the UV range. FTIR analysis showed the existence of O-Ti-O bond. XRD patterns indicated the presence of (101) and (112) plane crystalline phases of TiO_2. TEM images showed a spherical-like structure of TiO_2 NPs with various size distributions depending on the ablation period. The antibacterial activity of TiO_2 NPs was evaluated with different species of bacteria such as Escherichia coli, Pseudomonas aeruginosa, Proteus vulgaris, and Staphylococcus aurous, using the liquid approach. The optimum activity of TiO_2 NPs is found to be against E. coli at 1000 μg mL−1. Furthermore, adding, TiO2 NPs (1000 μg mL−1) in the presence of amoxicillin has a synergic effect on E. coli and S. aureus growth, as measured by the well diffusion method. However, both E. coli (11.6 ± 0.57mm) and S. aureus (13.3 ± 0.57mm) were inhibited [101].

In 2021, Kadhum and et.al explored the structural and fluorescence properties of titanium dioxide/silver (TiO_2/Ag) nanoparticle bilayers. The researchers identified unique structural and fluorescence characteristics, suggesting potential applications in various fields, such as optoelectronics, sensing, and photocatalysis [102].

In 2021, Iordanova et.al presented findings on the modification of chitosan/silver nanoparticles thin films using ultra-short laser pulses. They found that this adjustment resulted in enhanced antimicrobial properties, potentially allowing for fine-tuning the antimicrobial activity of such films for various applications [103].

In 2022, Rafiq et.al found that chitosan hydrogel loaded with Bischofia javanica could be an effective method for preparing stable, efficient silver nanoparticles with potent antibacterial properties. They suggested that these nanoparticles could have uses in medical treatments, environmental applications, and wound healing [104].

In2022, Alheshibri and et.al explored the synthesis of a composite material consisting of silver nanoparticles decorated on carbon nanotubes (CNTs) and titanium dioxide (TiO_2). The Ag/CNTs/TiO_2 nanocomposite showed excellent photocatalytic performance, suggesting its potential for environmental remediation applications [105].

In 2022, the researchers Ali and et.al prepared a three-layer nanocomposite containing silver, zinc oxide, and chitosan through laser evaporation. The nanocomposites displayed enhanced optical properties, antibacterial activity, and catalytic properties. The proposed strategy enables the growth of very fine Ag NPs (2–10 nm) with good dispersion, resulting in the synthesis of Ag/ZnO/Cs composites with antibacterial effectiveness, enhanced UV–visible barrier characteristics, and boosted catalytic reduction properties Staphylococcus aureus, Bacillus subtilus, Escherichia coli, and Pseudomonas aeruginosa are used to study the antibacterial activity of various Ag/ZnO/Cs hybrids. Within 10 min, Ag/ZnO/Cs exhibited 90 % removal efficiency after four cycles, demonstrating the efficiency and stability of the composite catalyst in reduction procedures. These nanocomposites might be effective in various applications [106].

1-13 The Aim of The Study

1- Fabricate a (CS-TiO_2-Ag) nanocomposite for the first time by using a pulsed laser ablation method.

2- Study the optical and structural properties of the manufactured material ((CS-TiO_2-Ag) nanocomposite).

3- Apply the (CS-TiO_2-Ag) nanocomposite: a) in killing two types of bacteria (*E. coli* and *Klebsiella*) and b) purifying contaminated water with high efficiency.

2.1 Introduction

This chapter covers knowledge of the optical properties of nanoparticles from UV-VIS spectroscopy, the absorption coefficient as well as the direct energy gap, compositional properties of nanoparticles as determined by energy-dispersive X-ray spectroscopy (EDX), structural properties involving infrared spectroscopy (FTIR), X-ray diffraction (XRD) imaging, scanning electron microscopy (SEM) and transmission electron microscopy (TEM) in addition to performing biological tests for bacteria, such as killing and inhibition tests, and testing of nanomaterials in water purification.

2.2 Optical Properties

2.2.1 Absorbance

Absorbance, also known as the absorbance rate, is a fundamental physical property that characterizes a material's ability to absorb energy from radiation, including light. This property is influenced by various factors, such as the material's composition, temperature, state (solid, liquid, or gas), and the type and energy of the radiation that it encounters. The concept of absorbance is often categorized based on different wavelength regions, such as ultraviolet, visible light, and infrared, which is especially significant in applications dealing with specific types of radiation, like solar energy techniques or spectroscopy [107].

Nanomaterials exhibit distinct absorbance characteristics compared to larger materials due to their unique properties at the nanoscale. The optical behavior of nanomaterials is influenced by factors such as particle size, shape, composition, and inter-particle interactions. For instance, silver nanoparticles appear yellow when suspended in water, while bulk solid silver appears leaden. This phenomenon is attributed to surface Plasmon resonance effects, which occur when electrons on the

nanoparticle's surface vibrate at a specific frequency due to their interaction with light [108].

The relationship between absorbance and the intensity of incident light, as well as the absorbing material, is crucial to understanding light-matter interactions. When light passes through a material, its portion is absorbed as a result of interactions with the material's molecules or atoms. Consequently, the intensity of the incident light that passes through the material decreases. This relationship is mathematically represented by the equation [109]:

$$A = \log(I_o/I) = -\alpha\, c\, x \quad \text{.....(2-1)}$$

$$I = I_o * e^{\wedge}(-\alpha\, c\, x) \quad \text{.....(2-2)}$$

Where

- A is the Absorbance
- I is the intensity of the transmitted light
- I_0 is the initial intensity of the incident light
- α is the absorption coefficient (a measure of the material's ability to absorb light)
- x is the thickness of the material.
- C is the Concentration of solution(M)

2.2.2 Absorption Coefficient

Absorption coefficient describes the ability of a material to absorb light as it passes through it. The absorption coefficient is denoted by "α". This coefficient depends on the properties of the medium, the thickness of the material and its ability to absorb incident rays. In addition, it provides valuable information about the nature of

electronic transitions that occur within the matter. A high value of absorption coefficient (α) exceeding 10^4 cm^{-1} indicates direct electronic transitions between the valence and conduction bands.On the contrary, a low value of (α) less than 10^4 cm^{-1} indicates the occurrence of indirect electronic transitions between the valence and conduction bands [110].

$\alpha = 1/x \ln (I/I_0)$……(2-3)

The absorption coefficient (α) can be calculated using the following equation(2-3) law known as the Beer-Lambert law, which is strongly related to the effect of absorption on the intensity of light. According to this law, the absorption coefficient (α) depends on the change in light intensity before and after passing through the material [110] .

2.2.3 Energy Gap

The energy gap is the space between the valence band and the conduction band. As light interacts with matter, electrons can absorb energy from photons, prompting a transition from the valence band to a state of higher energy. A large energy gap makes it difficult for electrons to transition from the valence band to the conduction band, leading to the material behaving as an insulator. Conversely, a small energy gap allows electrons to jump easily from the valence band to the conduction one, rendering the material conductive [111]. In the context of nanomaterials, the energy gap can be significantly affected by the size of the nanoparticles. As the particle size is reduced to the nanoscale, the energy gap typically increases due to quantum effects. This is known as the quantum size effect [112].

One method of determining the energy gap in such materials is the application of the Tauc equation, a tool that monitors how the absorption coefficient changes with photon energy. The mathematical relationship in the Tauc equation [113]. is given by:

$\alpha h\nu = A(h\nu - Eg)^r$ …….(2-3)

where

- h is the Planck constant.
- v is the frequency.
- r is a coefficient dependent on the type of allowed transitions.
- A is a constant dependent on the semiconductor details.
- Eg is the energy gap.

Generally, as the photon energy increases, so does the absorption coefficient, reflecting the increasing ability of photons to liberate electrons. By graphing this equation, the energy gap can be determined from the distance on the x-axis from the origin to the point where it intersects with the straight line [114].

2.3 Structural properties

2-3-1 Fourier transform infrared spectroscopy (FTIR)

Fourier analysis of infrared radiation (FTIR) is a widely used a chemical analysis tool. FTIR is used to determine the chemical composition of substances by measuring the interactions between molecules and infrared radiation. Infrared light is transmitted to the material, and the resulting spectra depend on the way infrared radiation is absorbed by molecules. This can be particularly useful in determining the chemical composition and chemical changes in a substance [115]. Table (2-1) shows the types of chemical bonds of the fluorescence spectrum[116].

When analyzing nanomaterials, interpretation of FTIR data can be more complex. Nanomaterials may cause infrared phenomena that are difficult to explain due to factors such as quantum interference and quantum mechanical perturbations. Therefore,

experience and advanced analytical software can be necessary to correctly interpret the data [117].

Table (2-1): For the fluorescence spectrum (FTIR)[116].

Type of Vibration			Frequency (cm^{-1})	Intensity	Page Reference
C—H	Alkanes	(stretch)	3000–2850	s	29
	$-CH_3$	(bend)	1450 and 1375	m	
	$-CH_2-$	(bend)	1465	m	
	Alkenes	(stretch)	3100–3000	m	31
		(out-of-plane bend)	1000–650	s	
	Aromatics	(stretch)	3150–3050	s	41
		(out-of-plane bend)	900–690	s	
	Alkyne	(stretch)	ca. 3300	s	33
	Aldehyde		2900–2800	w	54
			2800–2700	w	
C—C	Alkane		Not interpretatively useful		
C=C	Alkene		1680–1600	m–w	31
	Aromatic		1600 and 1475	m–w	41
C≡C	Alkyne		2250–2100	m–w	33
C=O	Aldehyde		1740–1720	s	54
	Ketone		1725–1705	s	56
	Carboxylic acid		1725–1700	s	60
	Ester		1750–1730	s	62
	Amide		1680–1630	s	68
	Anhydride		1810 and 1760	s	71
	Acid chloride		1800	s	70
C—O	Alcohols, ethers, esters, carboxylic acids, anhydrides		1300–1000	s	45, 48, 60, 62, and 71
O—H	Alcohols, phenols				
	Free		3650–3600	m	47
	H-bonded		3400–3200	m	47
	Carboxylic acids		3400–2400	m	61
N—H	Primary and secondary amines and amides				
	(stretch)		3500–3100	m	72
	(bend)		1640–1550	m–s	72
C—N	Amines		1350–1000	m–s	72
C=N	Imines and oximes		1690–1640	w–s	75
C≡N	Nitriles		2260–2240	m	75
X=C=Y	Allenes, ketenes, isocyanates, isothiocyanates		2270–1940	m–s	75
N—O	Nitro ($R-NO_2$)		1550 and 1350	s	77
S—H	Mercaptans		2550	w	79
S=O	Sulfoxides		1050	s	79
	Sulfones, sulfonyl chlorides, sulfates, sulfonamides		1375–1300 and 1350–1140	s	80
C—X	Fluoride		1400–1000	s	83
	Chloride		785–540	s	83
	Bromide, iodide		<667	s	83

2.3.2 Electron Energy Dispersive Technology (EDX)

Electron energy dispersive technology is an analytical technique widely used in X-ray techniques and electron microscopes to analyze the chemical composition of materials. This technique depends on the interaction between the electrons and the sample [118]. When EDX is used to analyze nanomaterials, information about the chemical composition of the material can be obtained at the nanometer level. This

requires the use of electron microscopy, which has a high-resolution emulsification capability [119] .

However, there are some limitations in using EDX for the analysis of nanomaterials. For instance, very thin samples may not produce a signal that is strong enough for elemental analysis. Additionally, analysis of nanoscale samples may be more complex due to the effects of size and shape on the signals produced [120]. For nanoscale samples, EDX technology can also be used in quantitative studies that require estimation of the relative proportions of chemical elements in a sample. This analysis requires knowledge of physical theories related to the production of X-rays and their interaction with the material [121].

To verify the accuracy of the results, the results of the EDX analysis are often compared with those of other analysis techniques, such as optical power dispersive (XRD) or XPS analysis [122].

2.3.3 X-Ray Diffraction (XRD)

Optical energy dispersive X-ray diffraction (XRD) analysis is a basic method used to characterize the crystal structure of materials. The basis of this technique is Bragg's law of diffraction, which assumes that X-rays are scattered from crystals in a pattern specific to the lattice crystal structure [123]. In the analysis of nanomaterials using XRD, information regarding the size and shape of nanocrystals can be obtained, along with determination of crystal structure and detection of any crystalline defects [124].

Bragg's law is an integral part of the XRD analysis, and it is expressed as follows [125]:

$2d \sin\theta = n\lambda$ ..... (2-4)

• d is the distance between the crystal planes.

• θ is the angle of incidence.

• n is an integer indicating the diffraction order.

• λ corresponds to the wavelength of the incident x-ray(1.5406A0).

When X-rays encounter a crystalline sample during an XRD analysis, they are deflected by the crystal planes. Each plane deviates from a part of the beam, as shown in figure (2-1), and the diffracted rays interfere with each other. If the path spacing of the rays is an integer multiple of the wavelength (described by Bragg's law), they overlap constructively. This phenomenon is known as Bragg diffraction. The direction of these diffracted rays and the resulting pattern provide important insights into the internal structure of the crystal [126].The crystal size (D) of the as-prepared materials, which plays an important role in material properties, can be estimated by X-ray spectroscopy and full width at half maximum (FWHM) by analyzing the following Scherrer equation [127]:

$$D = (0.9 * \lambda) / (\beta \cos(\theta))$$

where

- D is the crystal size
- FWHM is full width at half maximum (β)
- θ is the Brack angle

And 0.9 is a Scherrer constant called the form factor because it depends on the shape of the crystal.

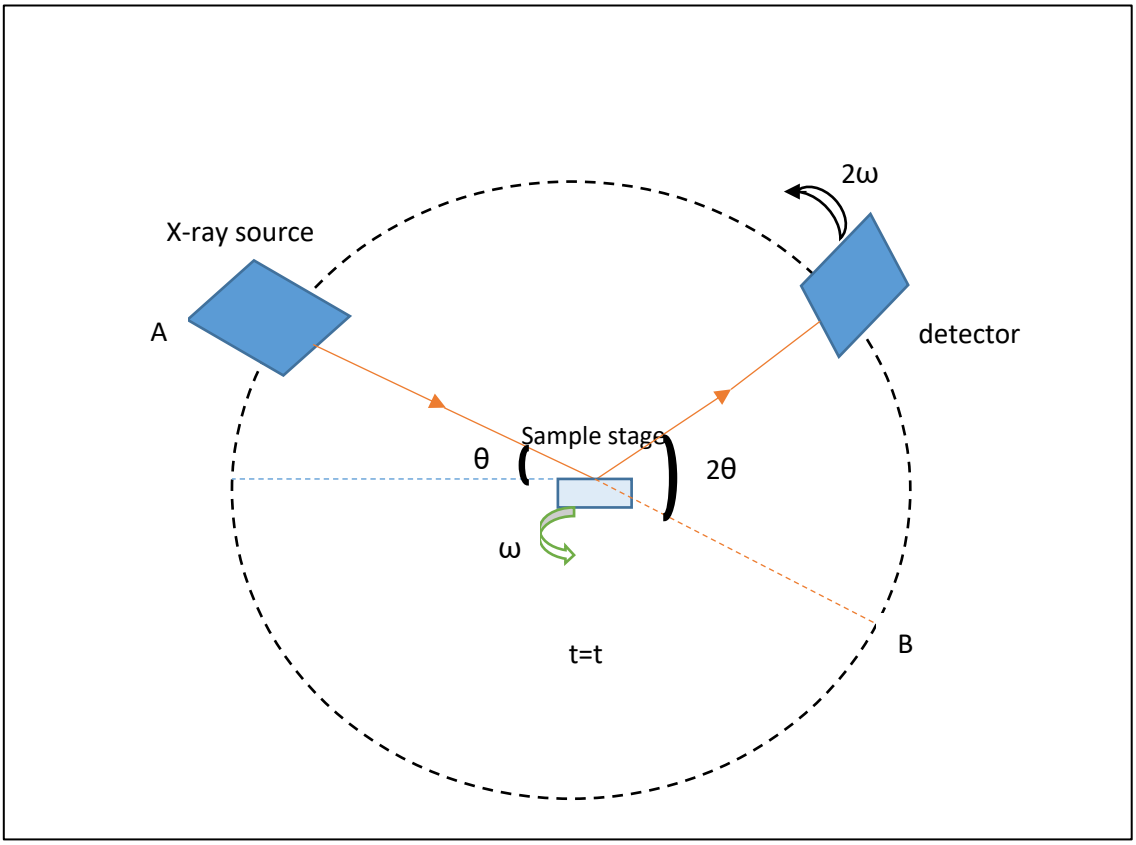

Fiqure (2-1): The X-Ray Diffraction (XRD) examination process

2.3.4 Scanning electron microscope (SEM)

The scanning electron microscope (SEM) is tool used in a wide variety of scientific and industrial applications. SEM is especially used to obtain high-resolution 3D surface images of samples with nanometer resolution. SEM works by creating a beam of electrons that is focused and directed toward a sample. When the electrons hit the sample, they excite the electrons in the sample and generate several signals that can be used to obtain information about the surface structure, chemical composition, and optical properties [128]. Figure (2-2) shows the SEM components [129]. In the case of nanomaterials, SEM can provide high-resolution images that show fine details of particle size, shape, and distribution [130].

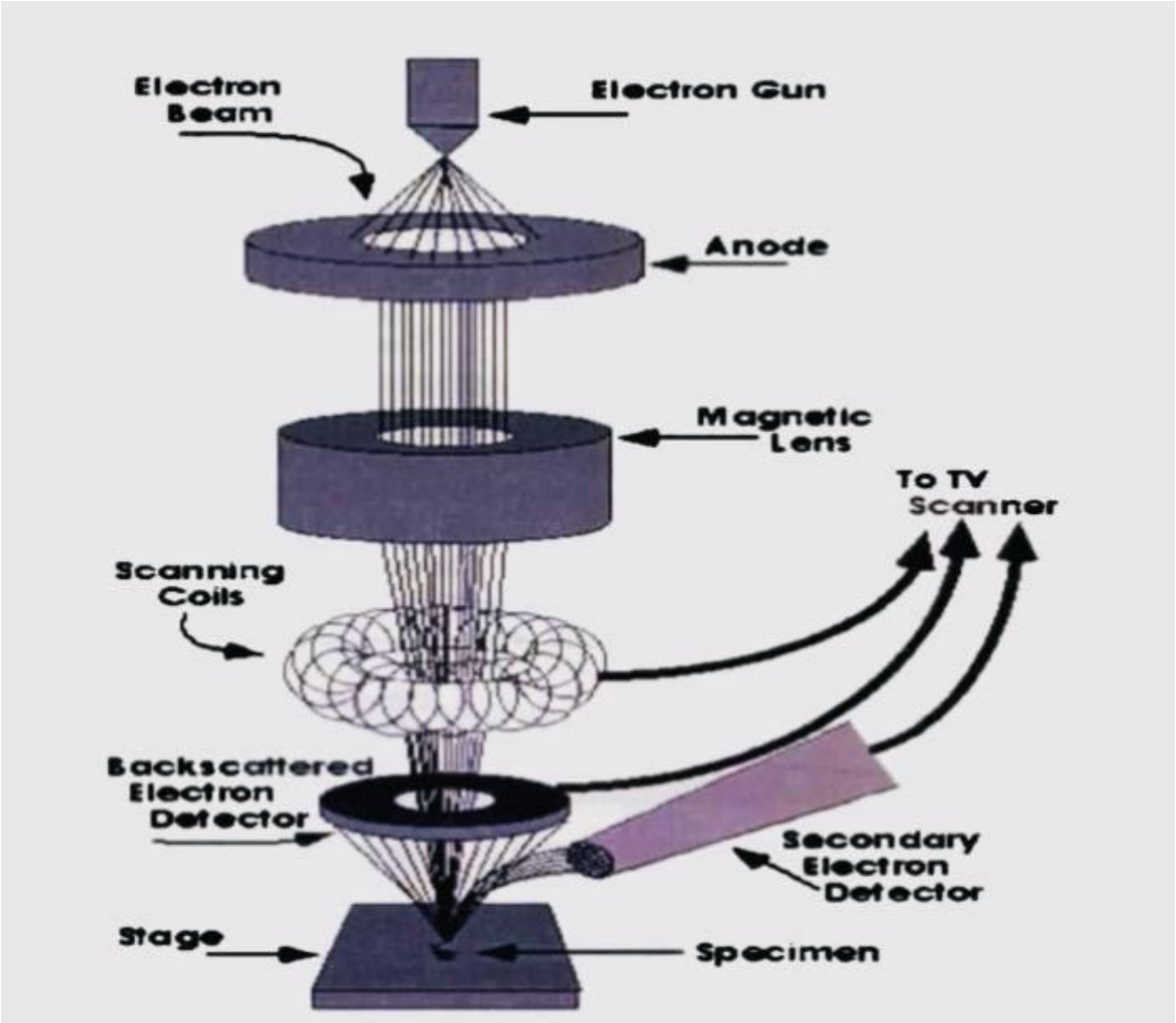

Figure (2-2): The SEM components [129].

2.3.5 Transmission Electron Microscope (TEM)

The Transmission Electron Microscope (TEM) is a type of electron microscope that utilizes a beam of electrons to illuminate the sample and generate an image. The beam of electrons is concentrated and directed across the sample using electrical and magnetic lenses .In a TEM, the sample consists of a very thin piece of material, transparent to the electrons. The electrons are accelerated and directed towards the

sample. Some of these electrons pass through the sample, while others are absorbed or scattered by the sample. A screen or detector that can generate a detailed image at the atomic level of the sample [131] captures the electrons that pass through the sample as shown in the figure (2-3) [129].

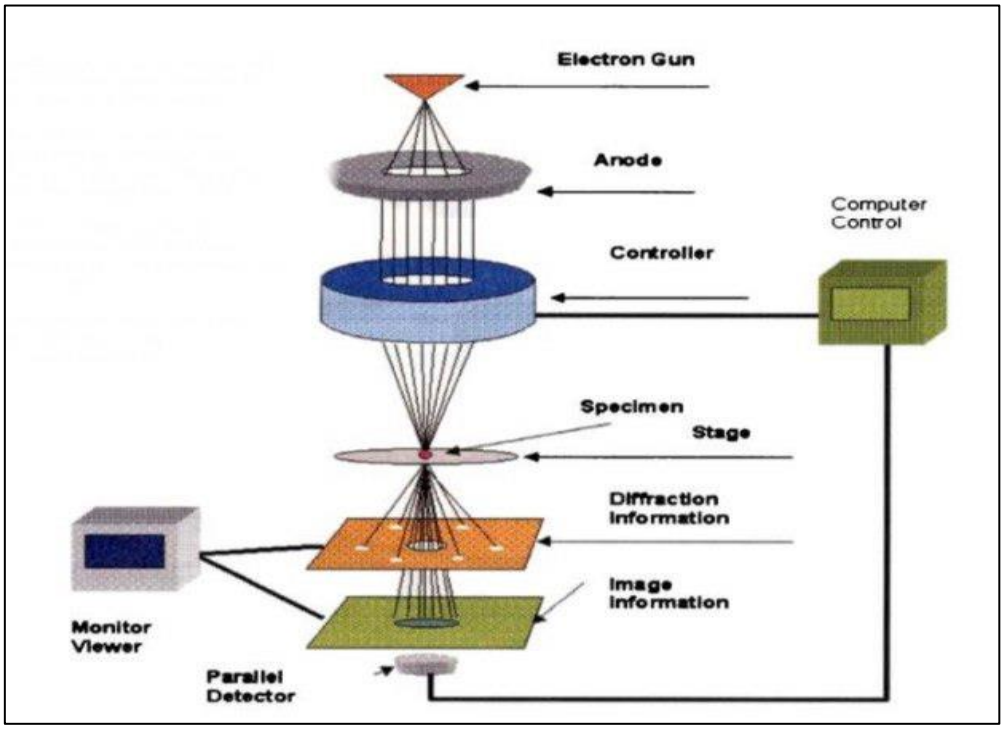

Figure (2-3):The TEM components [129].

TEM is utilized in a wide range of applications, additionally, the TEM can provide extremely high-resolution images up to the atomic level.

3.1 Introduction

This chapter demonstrates the preparation of nanomaterials, including Chitosan (CS), chitosan –Silver (CS-Ag), Chitosan -Titanium Oxide (CS-TiO_2), And Chitosan-Titanium Oxide -Silver (CS-TiO_2-Ag) by pulsed laser ablation in liquids using advanced analytical instrumentation. Measurements such as UV-vis spectroscopy, Fourier transform infrared (FTIR), energy dispersive X-ray spectroscopy (EDX), X-ray diffraction (XRD), scanning electron microscopy (SEM), and transmission electron microscopy (TEM) were calculated. The biological application of the prepared nanomaterials including eradication of E. coli and inhibition of Klebsiella bacteria, as well as their environmental application in the purification of polluted water, are explored.

3.2 Preparation of Nanomaterials

For the preparation of nanocomposites (CS-Ag, CS-TiO_2,and CS-TiO_2-Ag), titanium oxide and silver sheets were purchased from the commercial market and high-purity chitosan with a molecular weight of 1,500,000 g/mol from Life Sciences (GP5053).

To prepare the solution, 0.5 (g) of chitosan powder was taken by dissolving it in 670 ml of water and 70 ml of acetic acid [132]. A 5 ml of prepared chitosan solution was used to submerge a silver plate. The Department of Laser Physics, College of Science for Girls, University of Babylon, owns an Nd:YAG laser device. As shown in figure (3-1), it is manufactured in Germany to remove atoms from solid materials and extract them to form nanomaterials. With a wavelength of 1064 nm, an energy of 500 mJ, a pulse number of 500 pulses, and a frequency of 1 Hz. Then a silver plate was excised and a titanium plate was placed with the same parameters, but with a higher number of pulses (1000 pulses), Thus, the fabricating of CS-TiO_2-Ag. CS-Ag and CS-

TiO_2 nanocomposites were prepared separately in the same chitosan solution, and the same laser parameters mentioned before were used for CS-Ag, CS-TiO_2, and CS-TiO_2-Ag. These samples were deposited on aluminum blocks for EDX and SEM analysis. Additionally, the same samples were placed on a glass slide for XRD analysis. The liquid was used for analyses (UV-Vis, FTIR) and the liquid copper slide for (TEM).

Figure (3-1) : Pulsed Nd-YAG laser.

3.3 Devices That were Used.

Many devices were used in the measurements that were made on nanomaterials, as follows:

3.3.1 Absorption Spectrum Measurement (UV-Visible)

It is a device for measuring the absorbance of materials through a spectrometer that extends from 190 to 1100nm and was divided into three regions: 190-400nm ultraviolet spectrum, 400-750nm visible spectrum, and 750-100nm near infrared spectrum. This device is located in the College of Sciences for women, University of

Babylon, and its model is CECIL CE7200 UV-Visible as shown in figure (3-2). Through which the absorbance intensity of the nanomaterials prepared in this study was analyzed.

Figure (3-2) :UV- Spectrophotometer

3.3.2 Fourier Transform Infrared Spectrometer (FTIR)

It is used to find out the chemical bonds in the materials examined through FTIR spectroscopy by adding a few drops of solution shown in figure (3-3). The device was

operated at room temperature. The research was conducted in the Advanced Physics Laboratory at the College of Sciences for women, University of Babylon, made in Germany, with a model (ALPHAB).

Figure (3-3): Fourier Transform Infrared Spectrometer FTIR

3.3.3 X-ray Diffraction (XRD)

This device (type Analytical X 'Pert Pr), of British origin, as shown in figure (3-4) is used in order to know the characteristics of the crystal structure and the nature of crystal growth. The drop coating method prepared samples deposited on glass slides [133].

Figure (3-4): The X-ray diffraction (XRD) device.

3.3.4 Scanning Electron Microscopy (SEM), X-Ray Energy Dispersive Spectroscopy (EDX)

The size of the particles, their shapes, and the prepared nanostructures were studied by using a scanning electron microscope, where the samples to be examined were deposited on aluminum slides. An X-ray energy dispersive spectroscopy device is attached to scanning electron microscopy device, where it was examined to ensure the purity of the materials used. Figure (3-5) shows the associated SEM device with The EDX device, which are of American origin, are produced by the FEI Company located in the College of Pharmacy, University of Babylon.

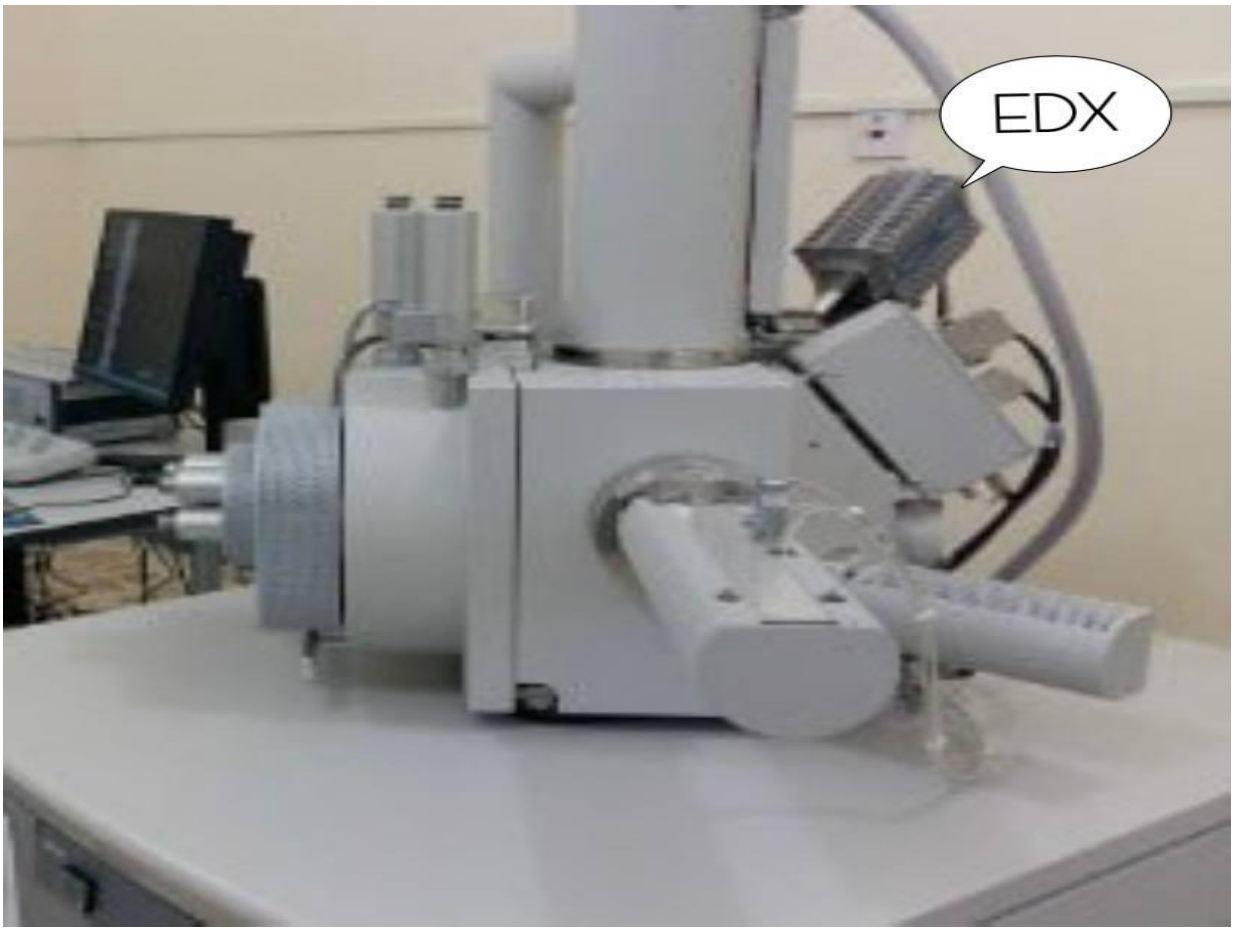

Figure (3-5): The scanning electron microscopy (SEM), energy dispersive X-ray (EDX)

3.3.5 Transmission Electron Microscopy (TEM)

It is an instrument used to analyze and characterize the size, shape, and atomic arrangement of nanomaterials [134]. The samples, which were deposited on a copper mesh, were analyzed using a German-made ZEISS LEO 912 model device, as depicted in figure (3-6).

Figure (3-6): The Transmission Electron Microscopy (TEM)

3.4 Biological Application

To apply the nanomaterials to killing bacteria, *E. coli* and *Klebsiella* bacteria were taken from the life sciences laboratories in the College of Sciences for Women, University of Babylon. To prepare Mueller-Hinton agar (a culture medium for bacteria), approximately 38 g of agar powder (CM0337B) is suspended in 1 L of distilled water. Then mix well and dissolve. Steam sterilises at 121 °C for 15 minutes. The liquid is then poured into a Petri dish and left to solidify. The surface of the agar plate is inoculated in the same way as the disc spread method, by spreading a volume of microbial inoculum over the entire surface of the agar. Then, using a sterile drill, a hole 6 to 8 mm in diameter is aseptically drilled, a volume (0.5 mL) of antibacterial nano-solution is applied, and then the agar plates are incubated at 37 °C. The

antimicrobial drug is spread into the agar medium, which inhibits the growth of the tested microbial strain [135].

3.5 Environmental Application

To purify polluted water taken from polluted sewage (Al-Yahudiyah Water stream) in Babil Governorate. A filter was made by the use of a sponge 5 cm long and 3 cm in diameter which was placed inside a 12 cm long syringe. The intravenous (IV) infusion set is then inserted into the bottom of the syringe, while the other end is placed in the cup, as shown in figure (3-7). Before the filtration process, the intensity of absorption of contaminated water was examined with a UV spectrometer.

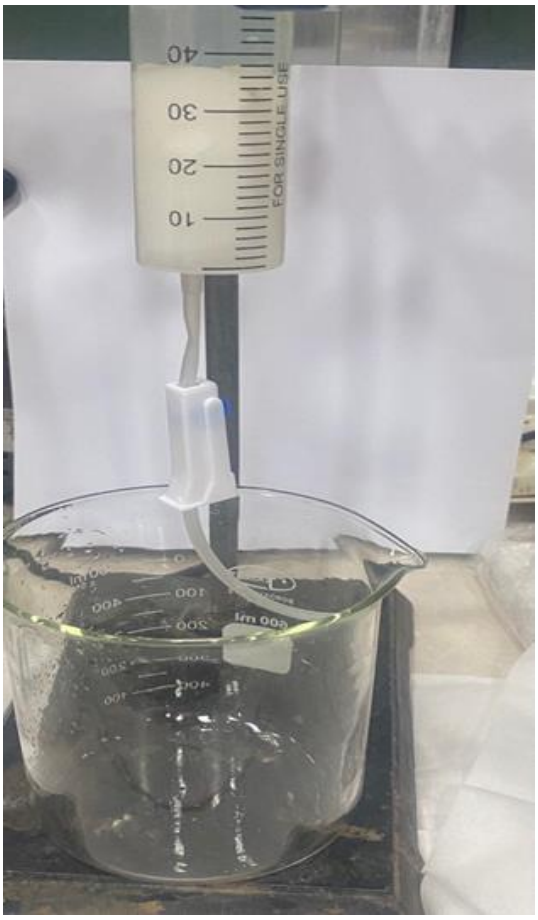

Figure (3-7): A water purification filter

The absorbance of contaminated water was measured after it was extracted. After passing the water through the produced filter, the absorbance was measured. After that, the sponge was submerged for five minutes inside the nanocomposite made of silver, titanium oxide, and chitosan, and the absorbance was measured. After refiltering the water and measuring its absorbance, the procedure was repeated, but this time, the combination was left inside the sponge for an additional five minutes before the absorbency was checked.

4.1 Introduction

This chapter presents the results of physical analysis of the optical properties (UV-Vis, absorption coefficient, gap energy), structural properties (FTIR, EDX,XRD , SEM and TEM) of the prepared nanocomposites (Cs),(Cs-Ag), (Cs-TiO_2) and (Cs-TiO_2-Ag) by pulsed laser ablation in liquid (PLAL). From the biological side, this chapter studies the effect of these compounds in killing *Escherichia coli* bacteria and inhibiting *Klebsiella* pneumonia. From the environmental side, this chapter shows how to filter and purify polluted water and discuss the results obtained.

4.2 optical properties

4.2.1UV-Vis absorption

UV-Vis septum a chitosan edge appeared at 275 nm, the peak of CS-Ag is at 400 nm, and for CS-TiO_2, the edge is at 375 nm. For CS-TiO_2-Ag, the peak position has no change, but the intensity of absorption had been changed due to the increasing in the concentration of nanoparticles in the solution [135,136], where the increment in the intensity of (CS-TiO_2) and the decreasing of (CS-Ag) intensity of the composite (CS-TiO_2-Ag). This is due to the presence of core-shell, which means that the silver is surrounded by titanium [137] as shown in figure (4-1).

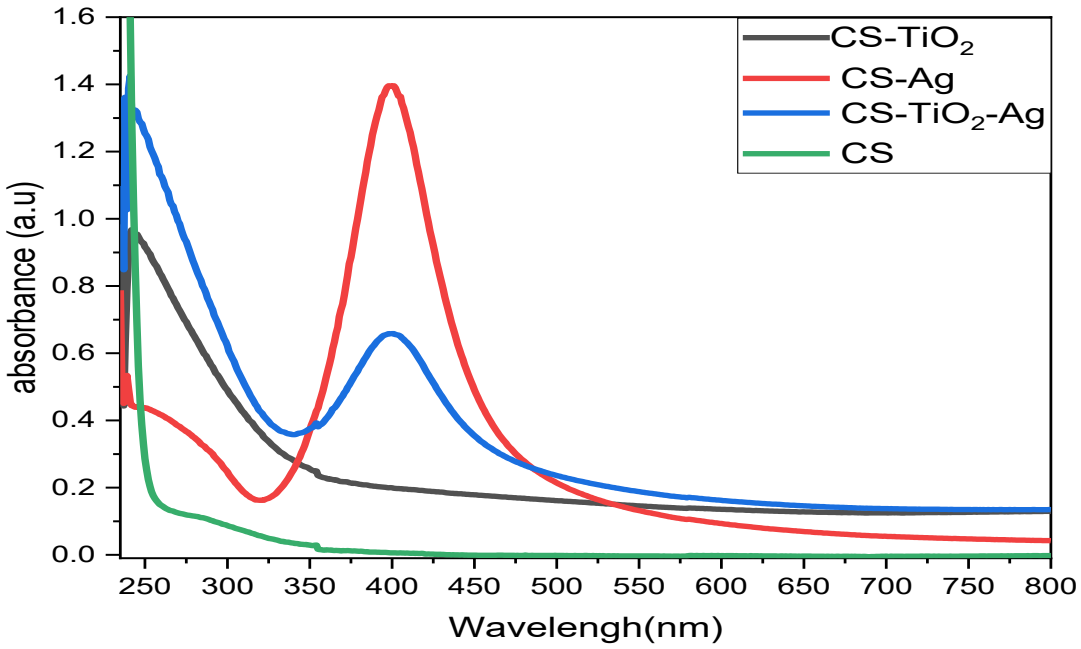

Figure (4-1): UV–vis spectra of the CS –Ag, CS-TiO_2, CS-TiO_2-Ag, and CS.

4.2.2 Absorption coefficient

Figure (4-2) shows the absorption coefficient at CS,CS-TiO_2,CS-Ag, and CS-TiO_2-Ag.The absorption coefficient values are shown in the table (4-1).

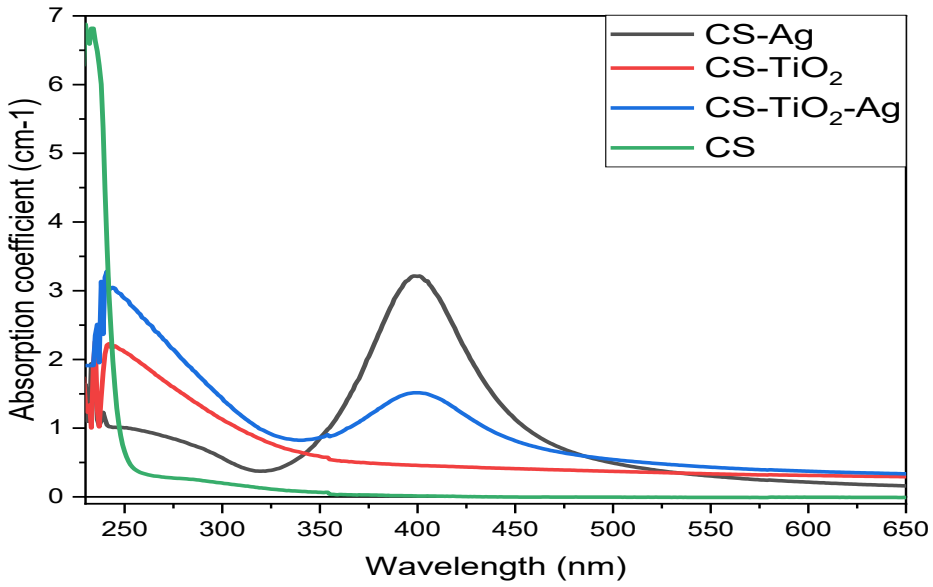

Figure (4-2): The absorption coefficient for CS, CS-Ag, CS-TiO_2, and CS-TiO_2-Ag

Table (4-1): The absorption coefficient for CS, CS-Ag, CS-TiO_2, and CS-TiO_2-Ag

nanocomposites	**absorption coefficient**(α) cm^{-1}	Wavelength (λ)(nm)	Ref.
CS	6.8	275	[138]
CS-Ag	3.3	400	[139]
CS-TiO_2	2.3	375	[140]
CS-TiO_2-Ag	CS-Ag (1.5),CS-TiO_2-Ag(3.2)	400, 375	[139,140]

4.2.3 Energy Gaps

The energy gaps of the {(Ag), (TiO_2), (CS), (CS-Ag), (CS-TiO_2), (CS-TiO_2-Ag)} as shown in figure (4-3). The values of the indirect energy gap are shown in the table (4-2). Titanium oxide is a semi-conducting oxide. When it is doped with chitosan polymer, it creates secondary levels in the energy gap between the valence band and the conductive band, as similar with silver nanoparticles.

Table (4-2):Direct energy gap for (Ag), (TiO_2), (CS), (CS-Ag), (CS-TiO_2), (CS-TiO_2-Ag)}

Nano material	Energy gap (ev)
Ag	1.6
TiO_2	2.5
CS	2.9
CS-Ag	2.37
CS-TiO_2	2.38
CS-TiO_2-Ag	2.1

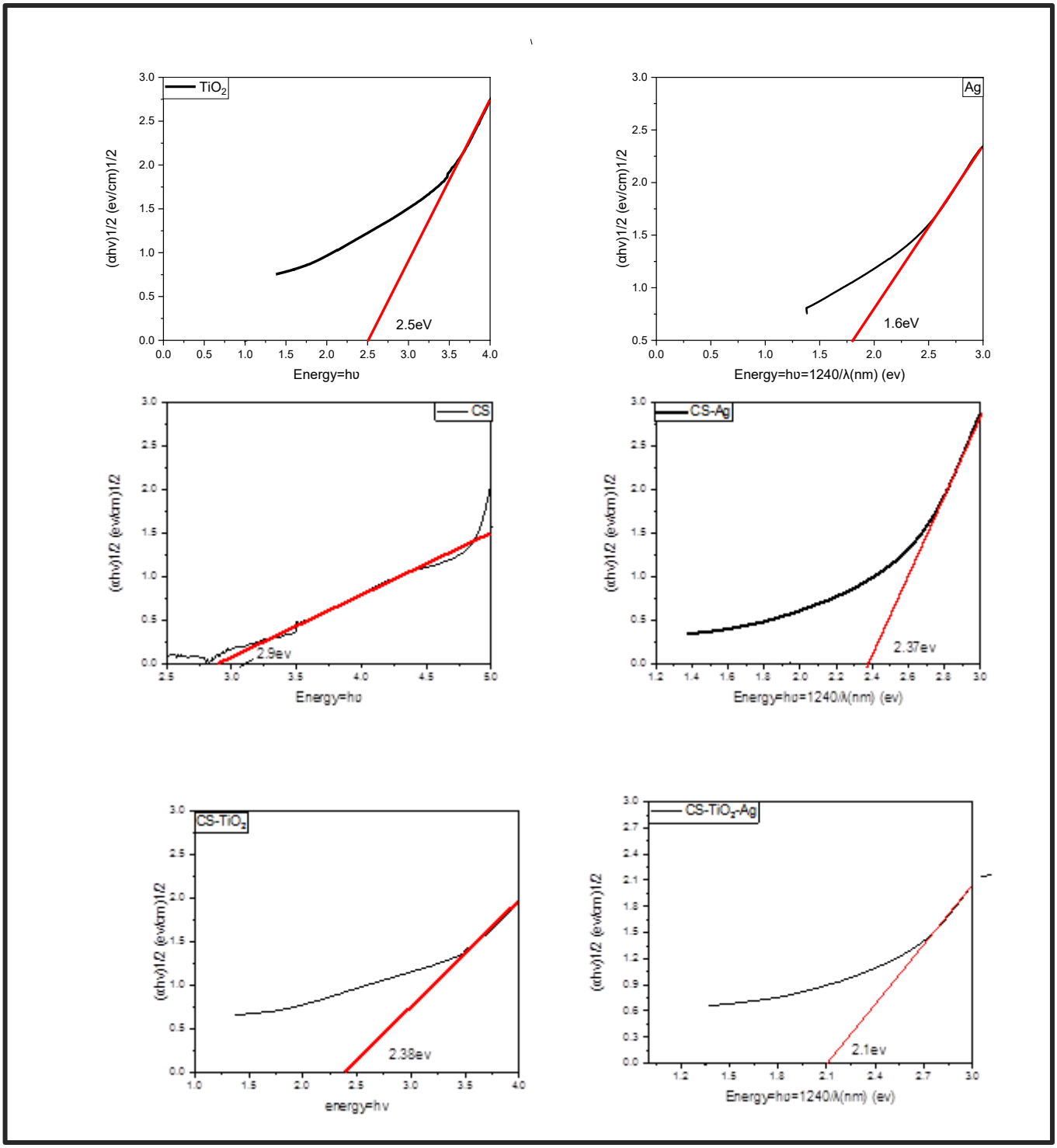

Figure (4-3): The energy gap (Ag), (TiO_2), (CS), (CS-Ag), (CS-TiO_2), (CS-TiO_2-Ag)

According to the previous results of the absorption coefficient of the prepared materials, it was proven that the energy gap of the prepared nanomaterials is a indirect gap.

4.3 Structural properties

4.3.1 Fourier Transform Infrared Spectrometer [FTIR]

infrared spectroscopy is a powerful tool for analyzing the functional groups present in molecules. In general, the position and shape of peaks in the infrared spectrum can be used to identify specific functional groups within the molecule [141].Figure(4-4) shows the chemical bonds (C-H, C-N, O-H, C-O, C-O-C, COO, C=H, C=C) to the chitosan polymer, which are present in all samples, and in the sample CS-Ag. Bonds (Ag-NH_2, Ag-O) follow the bond of silver with the polymer. In the sample, CS-TiO_2 bonds also appeared, indicating the presence of titanium in the polymer (Ti-O-Ti), the CS-TiO_2-Ag sample revealed links indicating the presence of both silver and titanium (Ag-O, Ti-O, Ti-C). These results indicate that the TiO_2 and Ag nanoparticles are present in the matrix of the CS polymer.

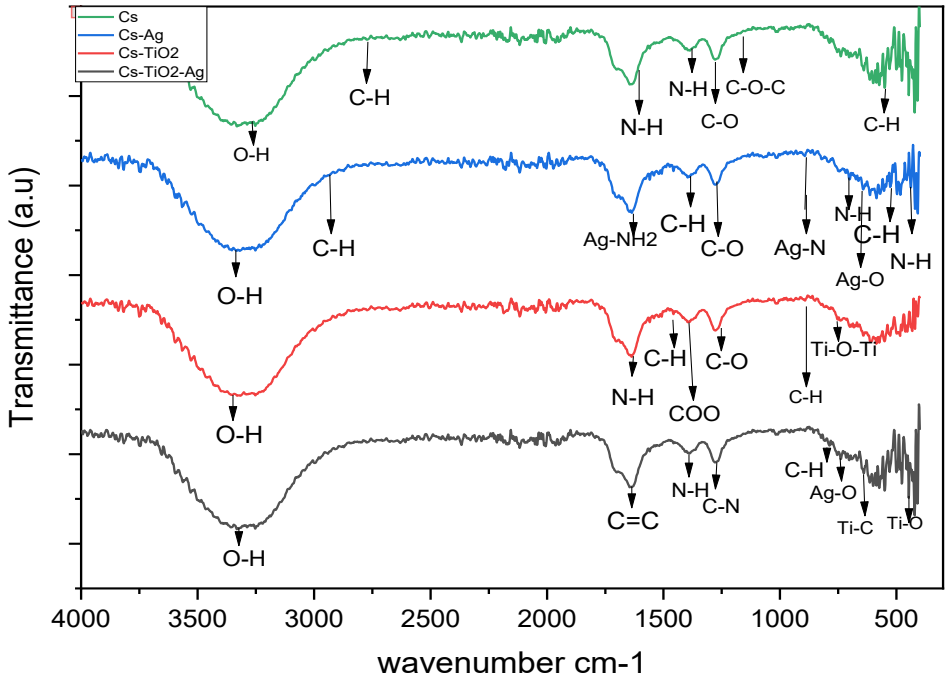

Figure (4-4): The FTIR for CS-Ag, CS-TiO_2, CS-TiO_2-Ag, CS.

4.3.2 Energy Dispersive X-Ray spectroscopy [EDX]

In the energy dispersive X-ray spectroscopy (EDX), as shown in figure (4-5A) and (4-5B), several elements such as (C, N, and O) are for chitosan [142,143]. Ag and Ti represent silver and titanium nanoparticles, and Al may be, Mo contaminated from the sample holder.

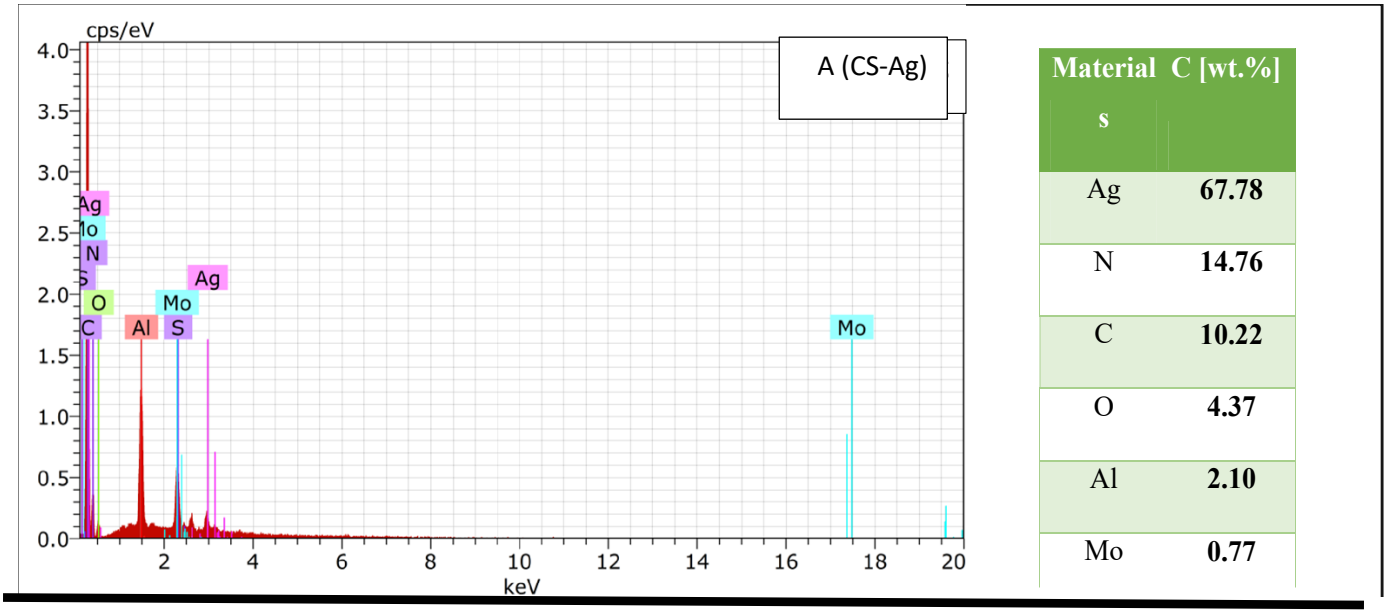

Materials	C [wt.%]
Ag	**67.78**
N	**14.76**
C	**10.22**
O	**4.37**
Al	**2.10**
Mo	**0.77**

Figure (4-5): The EDX for A(CS-Ag)

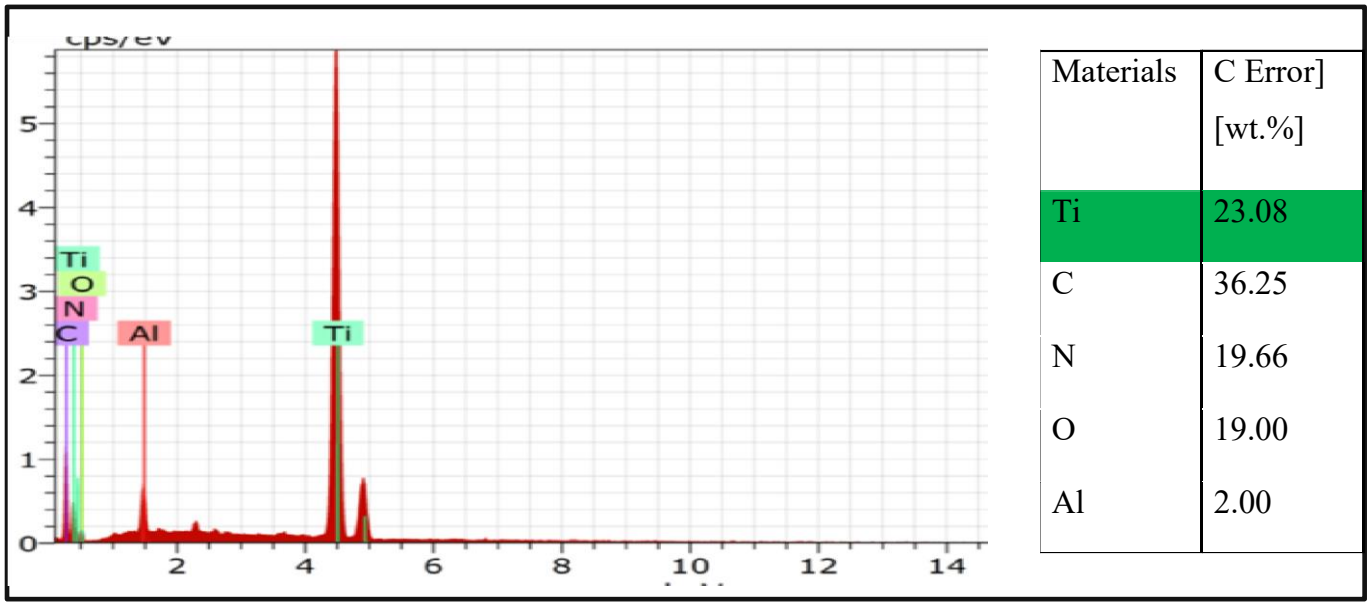

Materials	C Error] [wt.%]
Ti	23.08
C	36.25
N	19.66
O	19.00
Al	2.00

Figure (4-5): The EDX for B (CS-TiO_2)

4.3.3 X-Ray Diffraction [XRD]

X-ray diffraction technique was used to study the crystal structure of CS-TiO_2, CS-Ag and CS-TiO_2-Ag. In the diffraction spectrum, as in Figure (4-6), the chitosan polymer appears in the figure to have clear peaks at the angle (2θ = 10.5, 13.04) and in the direction [(020), (021)], respectively. This is consistent with a previous study [144], while in CS-TiO_2. It shows the peaks at (2θ = 29.701, 37.42), directions (101, 401), and intensities (110), (110), respectively. These angles coincided with the international card of titanium oxide (46-1238). The X-ray diffraction spectrum of CS-Ag shows the diffraction peaks at (2θ = 29.54, 32.03, 35.32, 37.27), corresponding to a previous study [145], the international card for silver (41-1402), and in the direction of (331), (131). , (100), (101) with density (100, 100, 20, 50) respectively.

In addition, for CS-TiO_2-Ag, its diffraction spectrum was at different angles (2θ = 29.655, 32.172, 37.328), directions (204), (404), (205) and density (150, 800, 100), respectively. , in comparison with the international card (32.1028).

The angles in CS-Ag, CS-TiO_2 were replicated with the CS-TiO_2-Ag angles, but the angles (29, 32, and 37) were different in intensity as described above.

The peaks for CS-Ag appeared more than the peaks for CS-TiO_2, although the number of pulses used in titanium ablation is more than the number of pulses used for silver, due to the higher bonding energy of titanium, as it needs a higher bonding energy. The number of pulses to eliminate bonds between its atoms [146,147].

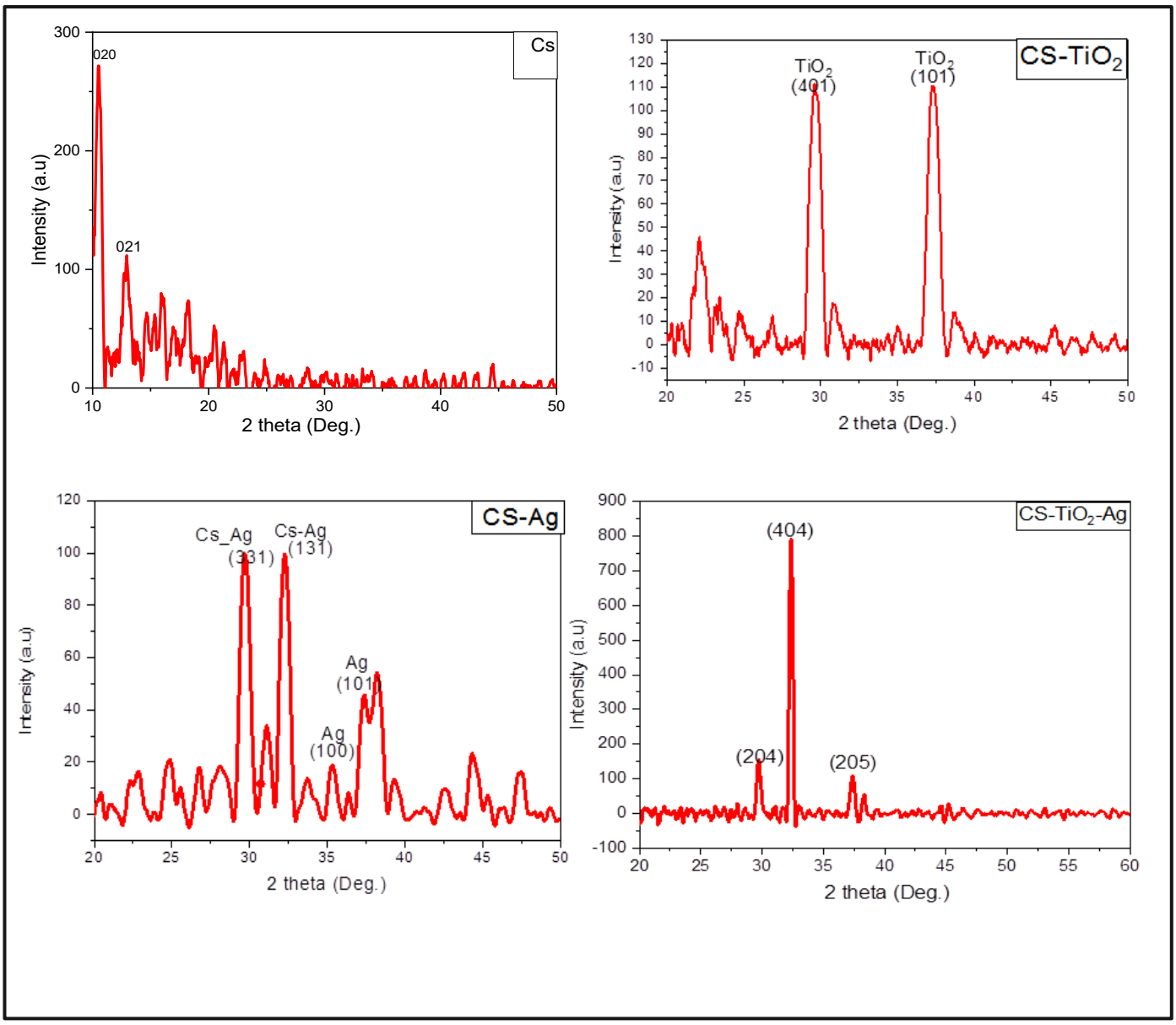

Figure (4-6): The XRD for (CS), (CS-TiO_2), (CS-Ag) and (CS-TiO_2-Ag)

4.3.4 Scanning electron microscope [SEM]

In the scanning electron microscope (SEM) images as in figure (4-7), sheet of chitosan formed with silver and titanium dioxide appeared in the form of white dots, and the grain size was different, the average particle size was 95 nm. Taking into account, the small sizes could not be calculated by the Imagej program.

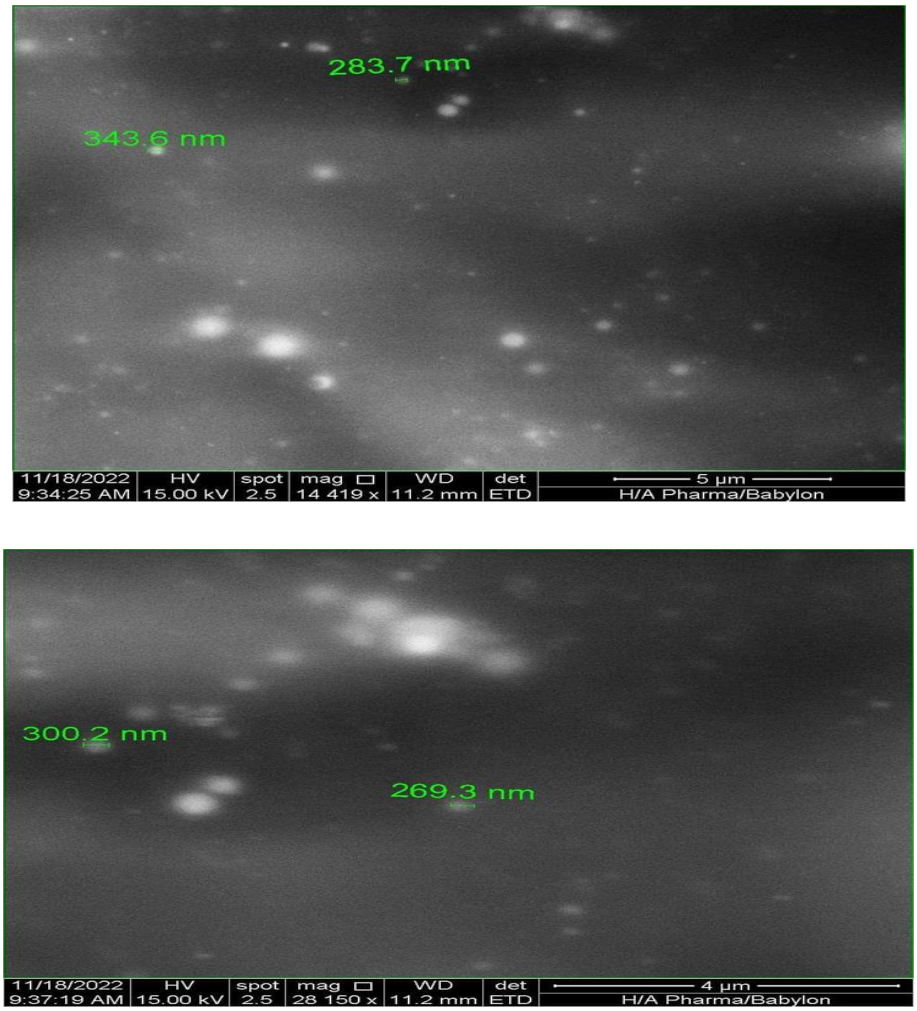

Figure (4-7): The SEM CS-TiO_2-Ag

4.3.5 Transmission electron microscopy [TEM]

The TEM image showed that chitosan is a heterogeneous particle in shape, whilst, generally, it is given a spherical appearance as in figure (4-8), chitosan usually shows a fibrous or plate-like structure. However, in the case of the observed particles, the chitosan polymer took on a spherical shape. The concentration of the polymer, in addition to other factors such as the method of preparation, temperature, and pH, affects the shape of chitosan [148]. It turns out that the average size is 13 nanometers, as shown in figure (4-9).

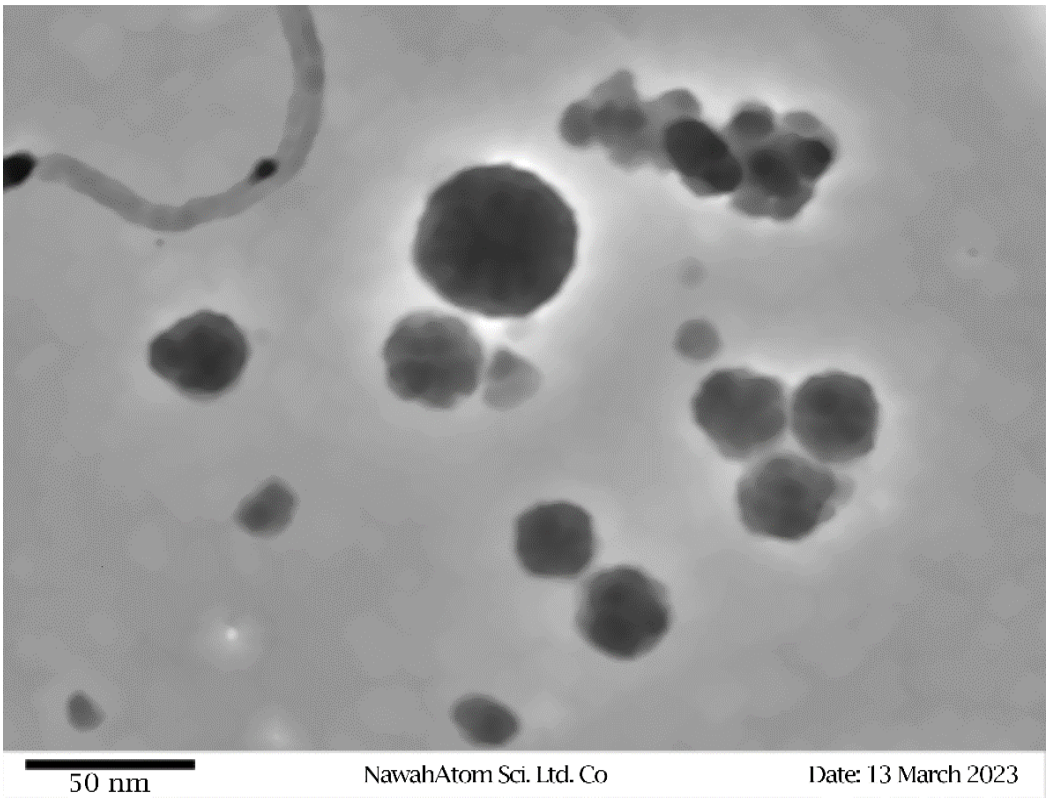

Figure (4-8): The TEM CS nanoparticle

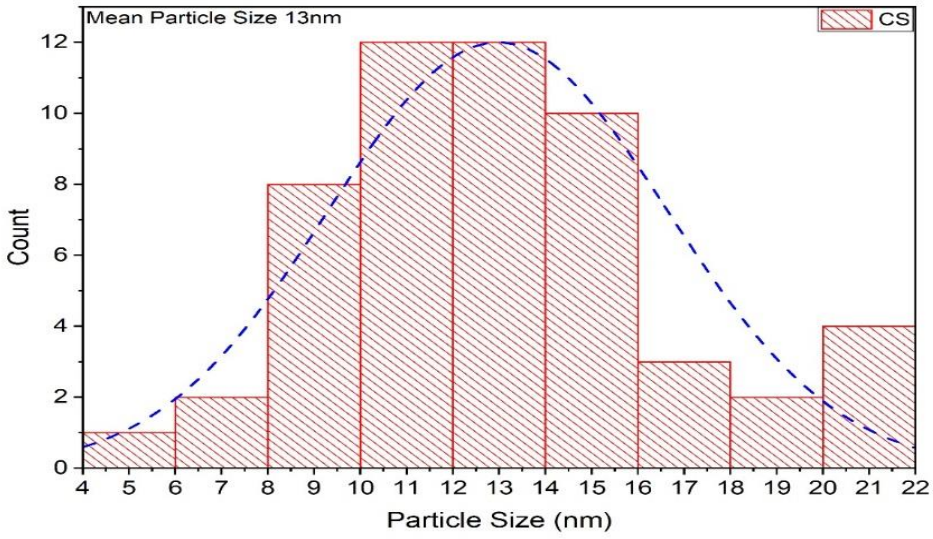

Figure (4-9): Diagram of the size of a CS nanoparticle

In the case of the nanocomposite (CS-Ag), the particles appeared to be almost spherical and in the shape of a core -shell, as in figure (4-10). The size of the nanoparticles is about 34 nm, as in figure (4-11). This is because the surface of the silver is covered with chitosan which acts as an encapsulating agent and can be deposited on the surface of the silver particles, leading to the formation of a core-shell structure with the core composed of silver and the shell composed of chitosan [149].

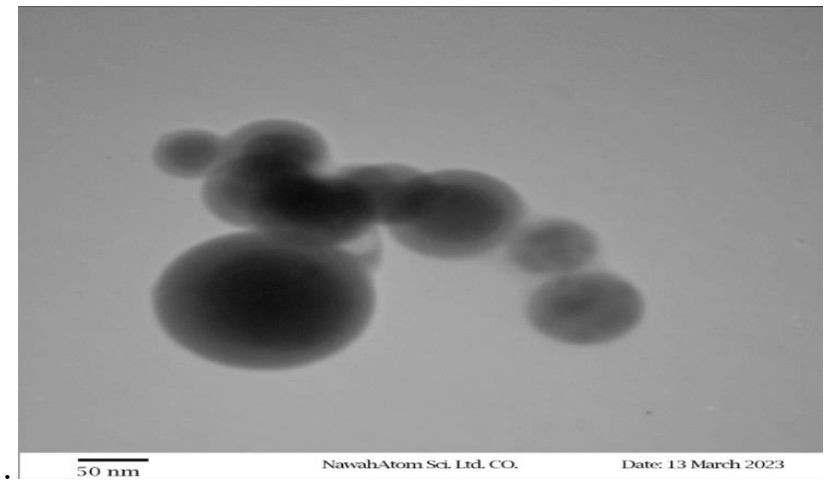

Figure (4-10): The TEM CS-Ag nanoparticle

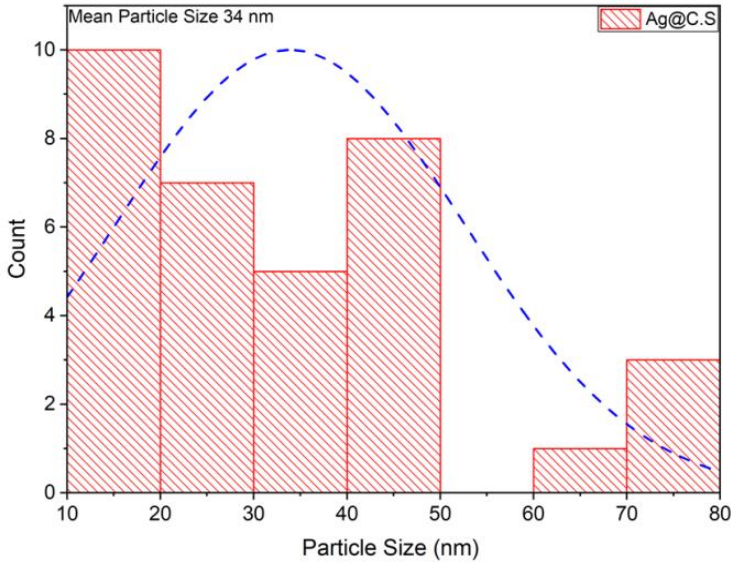

Figure(4-11): Diagram of the size of a (CS-Ag) nanoparticl

In the case of (CS-TiO_2), it appeared in a semi-spherical shape and was covered with spherical chitosan particles, as in figure (4-12). The average size of the nanocomposite (CS-TiO_2) is 15 nanometers, as shown in figure (4-13).

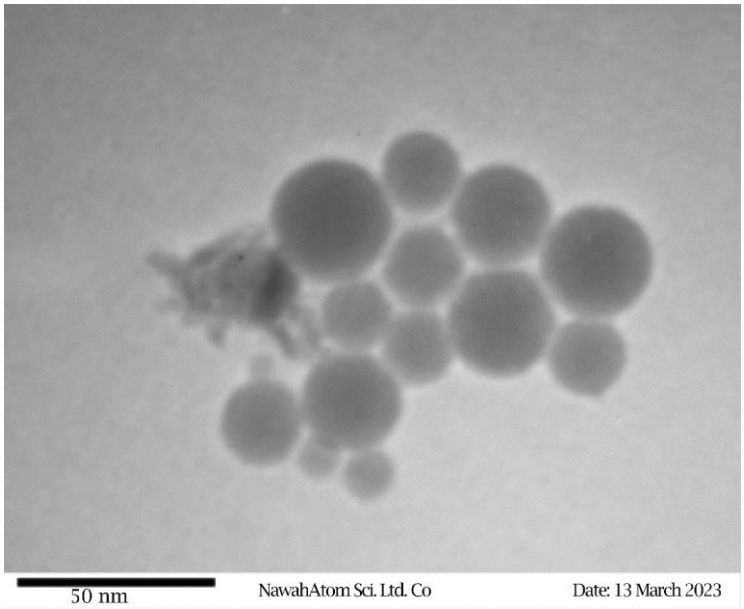

Figure (4-12): The TEM CS-TiO_2 nanoparticles

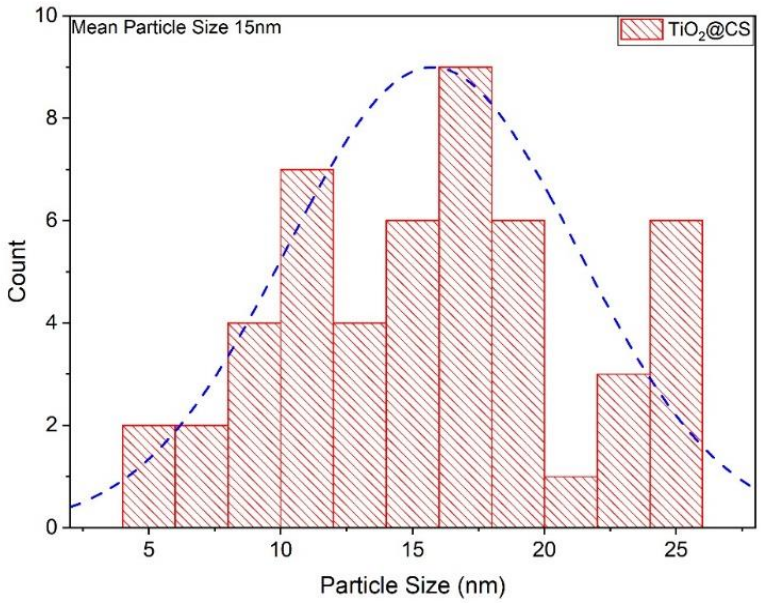

Figure(4-13): Diagram of the size of a CS-TiO_2 nanoparticle

In the case of the nanocomposite, it appeared in a spherical shape, as shown in figure (4-14). The effect of chitosan on silver nanoparticles and titanium oxide

nanoparticles can be varied and depends on the preparation conditions and concentrations used. The average size of the CS-TiO_2-Ag compound is 32nm, as shown in figure (4-15).

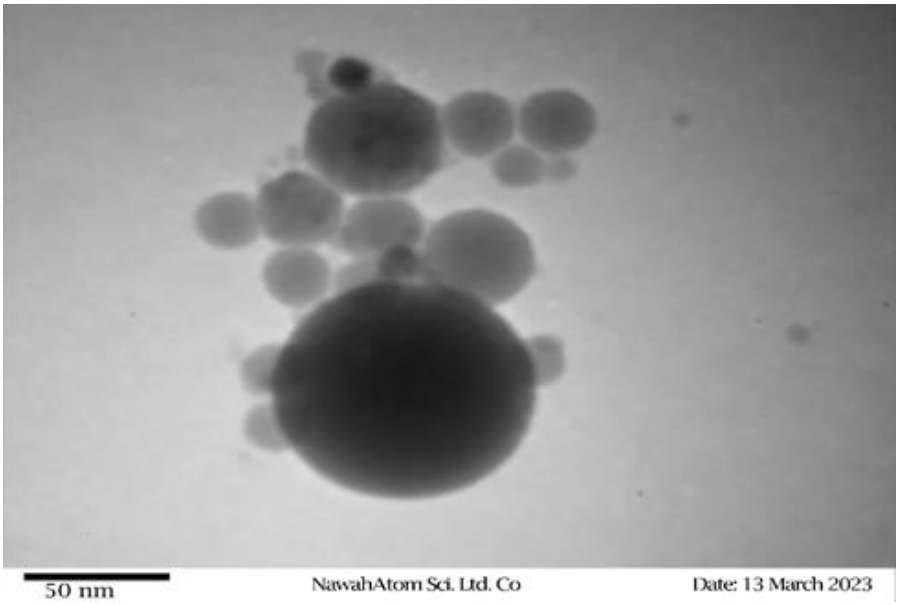

Figure (4-14): The TEM CS-TiO_2-Ag nanoparticles

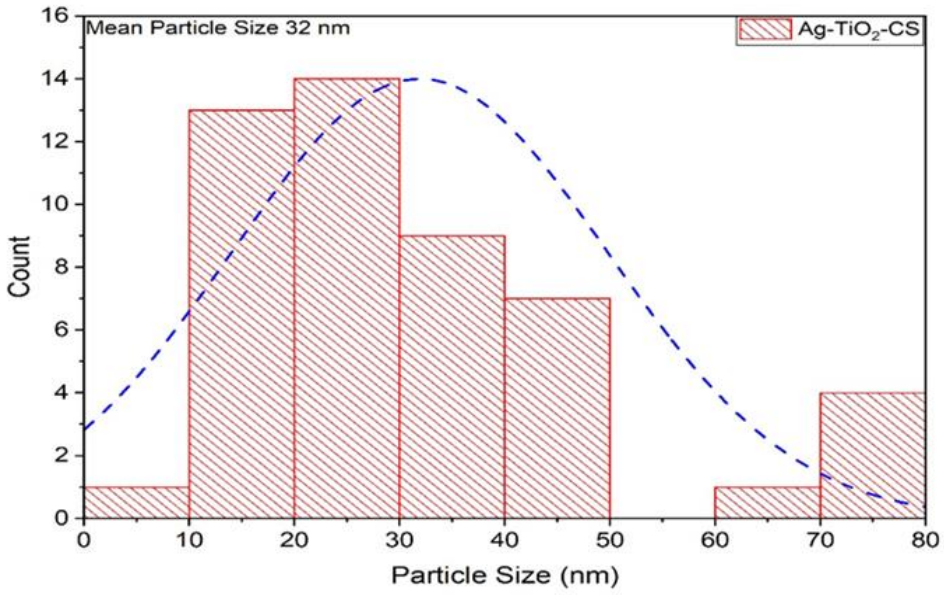

Figure (4-15): Diagram of the size of a CS-TiO_2-Ag nanoparticle

4.4 Nanocomposite applications

4.4.1 Antimicrobial applications

The *E.coli* bacteria were apply on various compounds, including CS, CS-TiO_2-Ag, CS-Ag, and CS-TiO_2, at a rate of 200 µl per compound. After an incubation period of 24 h at 37 °C, the highest killing rate of 40 mm was observed with the CS-TiO_2-Ag nanocomposite, followed by the CS-TiO_2 nanocomposite at 38 mm. The composite of CS-Ag exhibited a killing rate of 36 mm, while the CS polymer showed the lowest rate of 20 mm. These results are depicted in Figure (4-16). Additionally, after an incubation period of 72 h, the killing rates remained unchanged, confirming the complete elimination of the bacteria by the compounds.

Table (4-3): Area of killing zones for *E. coli* bacteria

Nano material	Killed *E.coli*
CS	20(mm)
CS-Ag	36(mm)
CS-TiO_2	38(mm)
CS-TiO_2-Ag	40(mm)

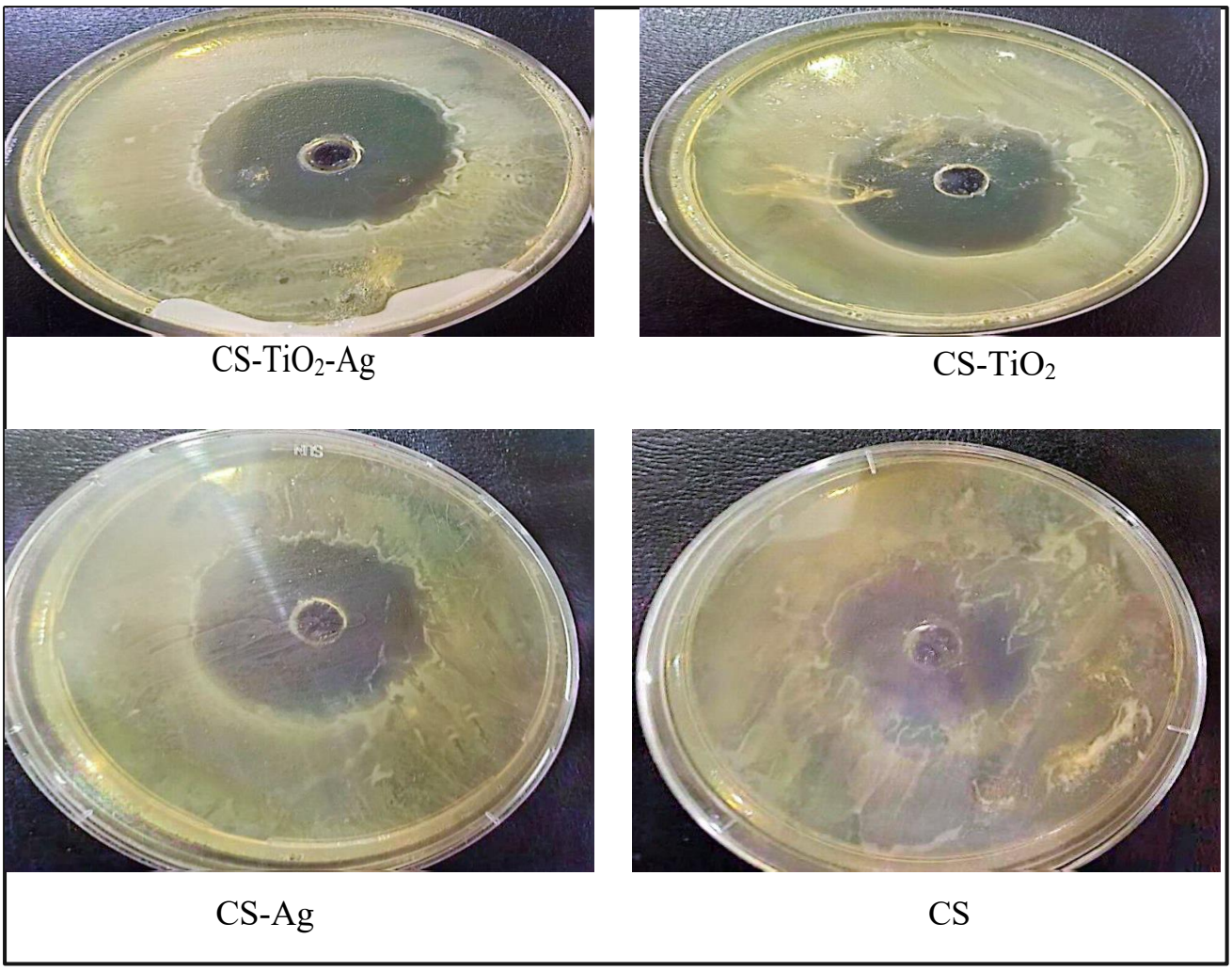

Figure (4-16): The killed the bacteria (*E.coli*)

When nanomaterials were added to *Klebsiella* bacteria under identical conditions for 24 h, the killing rates for CS-TiO_2-Ag, CS-TiO_2, CS-Ag, and CS were found to be 43 mm, 38 mm, 35 mm, and 28 mm, respectively, as illustrated in figure (4-17A). However, after an incubation period of 72 h, the bacteria were observed to regrow, as shown in figure (4-17B). These results indicate that the nanocomposites are able to inhibit *Klebsiella* bacteria and kill *E. coli* bacteria.This outcome can be attributed to the fact that E. coli bacteria carry a positive charge, whereas *Klebsiella* bacteria carry a negative charge.

Table (4-4): The inhibit zones *Klebsiella* bacteria

Nano material	inhibit *Klebsiella* bacteria
CS	28(mm)
CS-Ag	36(mm)
CS-TiO_2	38(mm)
CS-TiO_2-Ag	43(mm)

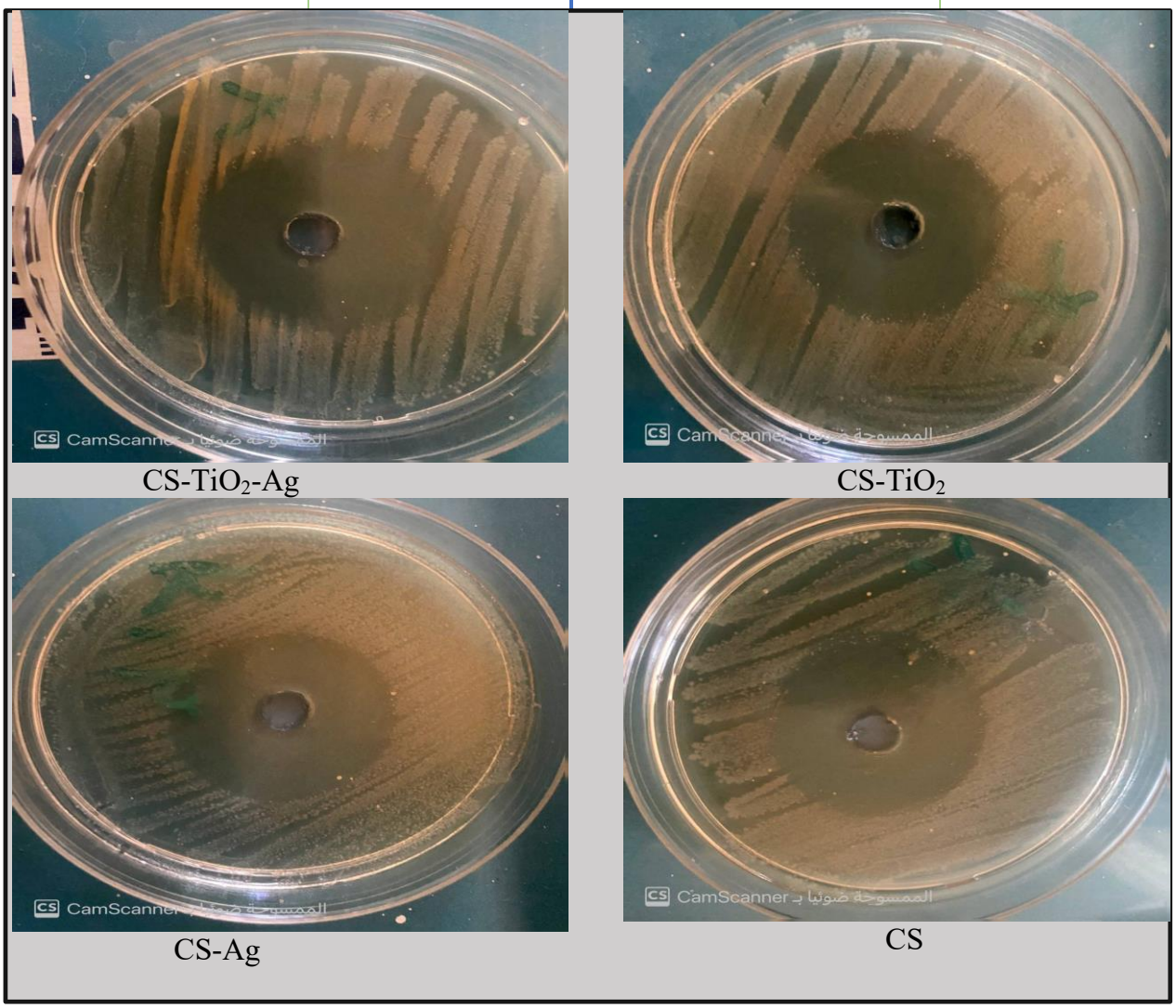

Figure (4-18A): The killed bacteria (*Klebsiella*)

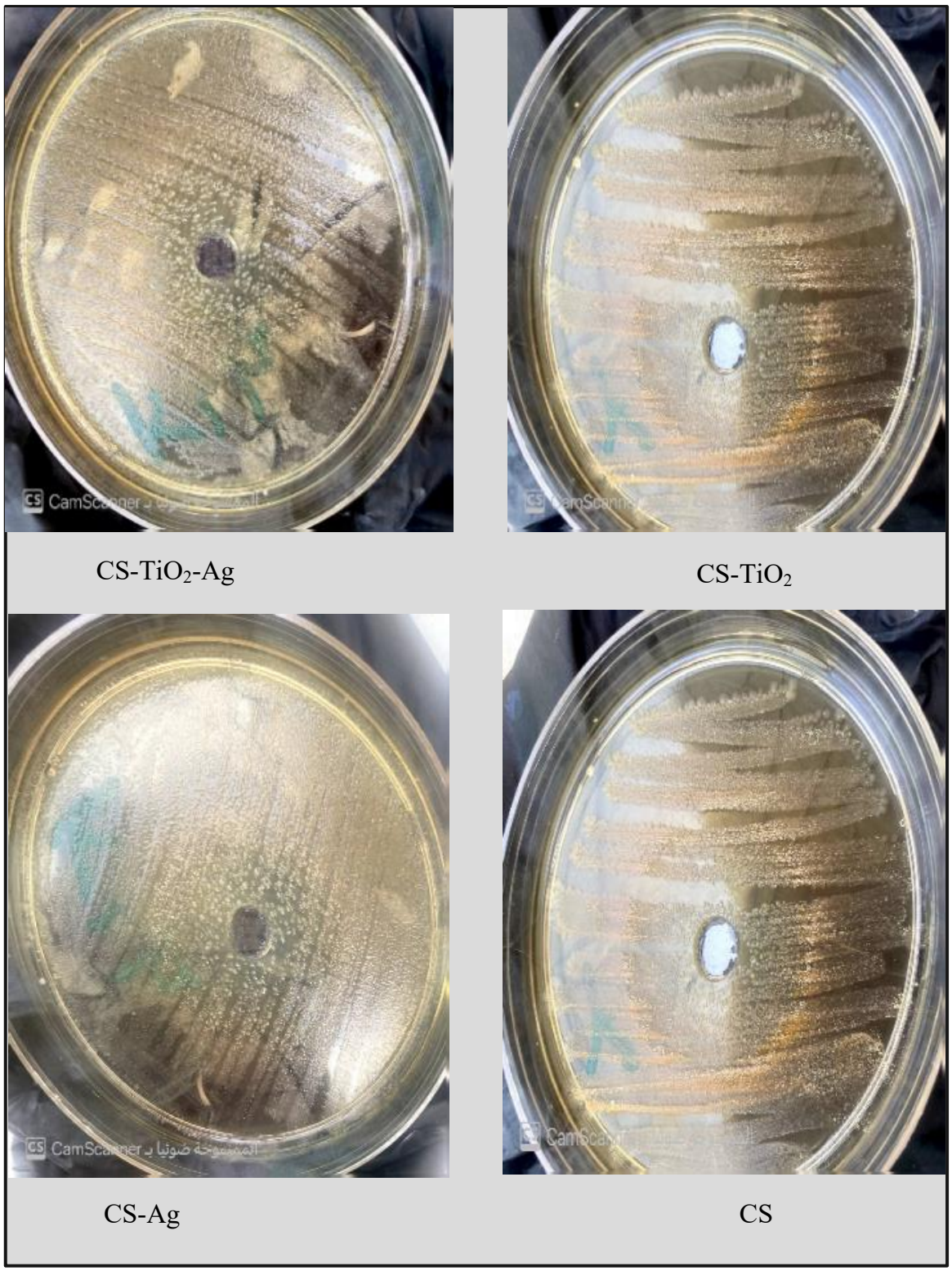

Figure (4-18B): The inhibited bacteria (*Klebsiella*)

Table (4-5): Compared with previous studies of the effect of nanocomposites in killing bacteria.

Nano material	Method of preparing nanomaterial	Type of bacteria	Killed rate	Ref.
CS-TiO_2	chemical method	E. coli	Kills E. coli bacteria 100% after 24 hours	93
CS-TiO_2- Cu	Sol-gel and ultra - sonication	E. coli and staphyloco	Completely killed	95
TiO_2	laser ablation technique	Escherichia coli, Pseudomonas aeruginosa, Proteus vulgaris, and Staphylococcus aureus	E. coli (11.6 ±0.57mm) and S. aureus (13.3 ± 0.57mm) were inhibited	101
CS-Ag_ZnO	laser evaporation	Staphylococcus aureus Bacillus subtilus, Escherichia coli	within 10 min exhibited 90 %	106
CS-Ag	chemical method	*E. coli and S. aureus*	More than 90% if the incubation hour is increased	150
CS-TiO_2-Ag	Puls laser ablation in liquid	Killed *Escherichia coli* and inhibited bacteria *(Klebsiella)*	Completely killed *Escherichia coli* and inhibited bacteria *(Klebsiella)*	Our study

4.4.2 Water Purification

The effectiveness of the filter shown in figure (4-19):

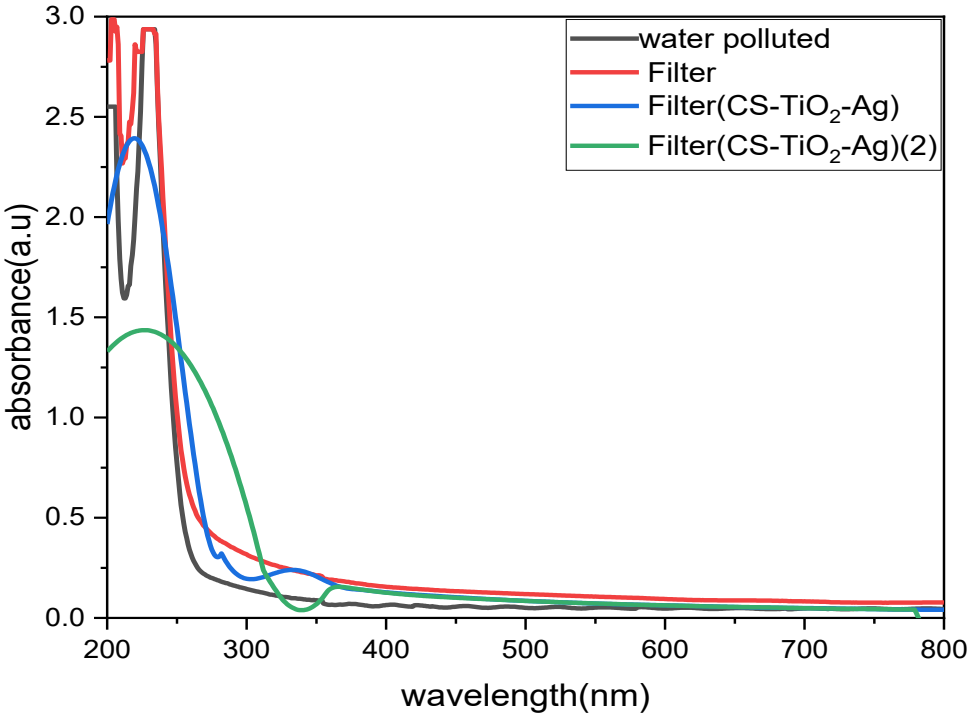

Figure (4-19): UV–vis spectra of the water polluted, sponge filter only, sponge filter with (CS-TiO_2-Ag).

for water purification was evaluated by measuring the adsorption of contaminated water. Initially, the absorption intensity was found to be 2.54. After the water is passed through the filter, it is found that the absorbance increases to 2.77, which indicates that the filter has successfully captured and removed pollutants. Then, the same process was repeated with the application of the nanoparticles after an interval of 10 minutes, and the absorbance was found to be 1.33, which indicates the continued efficiency of the filter in removing pollutants and the efficiency of the nanocomposite (CS-TiO_2-Ag) in removing pollutants.

Based on these results, it can be concluded that the filter is suitable for purifying water with an efficiency of 50%.

4.5 Conclusions

- Pulsed laser ablation in liquids has been demonstrated as an effective and safe method for preparing nanomaterials. This technique has been successfully used to create chitosan-based nanocomposites, indicating its ability to achieve nanostructures with precise control of properties.
- The energy band gaps of the as-prepared nanomaterials were successfully determined, and the absorption spectra provided clear details of the absorption peaks associated with the additives. The study confirmed the existence of the crystal structures through X-ray diffraction analysis, highlighting material compositions and crystal sizes.
- Nanoparticles have been shown to be effective against *Escherichia coli* and *Klebsiella* bacteria, which represents a major advance in infection control and public health.
- CS-TiO_2-Ag has demonstrated high water filtration efficiency, confirming its ability to improve water quality and positively impact the environment.
- This study lays a strong foundation for the use of nanomaterials across a variety of applications, including infection control and water purification, opening the door for further research and development in this fascinating field.

  In summary, the results of this study indicate a promising potential for employing the nanomaterials prepared using the pulsed laser ablation method in liquids to enhance various applications. This highlights their versatility in multiple areas, and showcases the ability to achieve tangible and effective improvements.

4.6 Future studies

1. Applying the nanocomposite (Chitosan-TiO_2-Ag) to other types of bacteria, parasites, or fungi.
2. Mixing chitosan polymer with magnetic materials and studying their properties.
3. Preparation of a nanocomposite containing chitosan in different concentrations and studying the changes in properties.

References

1- Aydın, Ahmet, Hande Sipahi, and Mohammad Charehsaz. "Nanoparticles toxicity and their routes of exposures." *Recent advances in novel drug carrier systems* (2012): 483-500.

2- Crosby, Alfred J., and Jong-Young Lee. "Polymer nanocomposites: the “nano” effect on mechanical properties." *Polymer reviews* 47.2 (2007): 217-229.

3- Huang, Wei, and Chenming Zhang. "Tuning the size of poly (lactic-co-glycolic acid)(PLGA) nanoparticles fabricated by nanoprecipitation." *Biotechnology journal* 13.1 (2018): 1700203.

4- Hyun, Yang H., et al. "Rheology of poly (ethylene oxide)/organoclay nanocomposites." *Macromolecules* 34.23 (2001): 8084-8093.

5- Ash, B. J., L. S. Schadler, and R. W. Siegel. "Glass transition behavior of alumina/polymethylmethacrylate nanocomposites." *Materials Letters* 55.1-2 (2002): 83-87.

6- Divya, K., and M. S. Jisha. "Chitosan nanoparticles preparation and applications." *Environmental chemistry letters* 16 (2018): 101-112.

7- Brinker, C. Jeffrey, and George W. Scherer. *Sol-gel science: the physics and chemistry of sol-gel processing*. Academic press, 2013.

8- Wang, Lawrence K., et al. "Chemical precipitation." *Physicochemical treatment processes*. Totowa, NJ: Humana Press, 2005. 141-197.

9- Pierson, Hugh O. *Handbook of chemical vapor deposition: principles, technology and applications*. William Andrew, 1999.

10- Abraham, Farid. *Homogeneous nucleation theory: the pretransition theory of vapor condensation*. Vol. 1. Elsevier, 2012..

11- Xiong, Hong-Bing, and Jian-Zhong Lin. "Nanoparticles modeling in axially injection suspension plasma spray of zirconia and alumina ceramics." *Journal of thermal spray technology* 18 (2009): 887-895.

12- Yadroitsev, Igor, Ph Bertrand, and I. Smurov. "Parametric analysis of the selective laser melting process." *Applied surface science* 253.19 (2007): 8064-8069.
13- Dell'Aglio, M., et al. "Mechanisms and processes of pulsed laser ablation in liquids during nanoparticle production." *Applied Surface Science* 348 (2015): 4-9.
14- Manasreh, Omar. *Introduction to nanomaterials and devices*. John Wiley & Sons, 2011.
15- Vollath, Dieter. "Nanomaterials an introduction to synthesis, properties and application." *Environmental Engineering and Management Journal* 7.6 (2008): 865-870.
16- Zhai, Tianyou, and Jiannian Yao. *One-dimensional nanostructures: principles and applications*. John Wiley & Sons, 2012.
17- Cheong, K. Y. (Ed.). *Two-dimensional nanostructures for energy-related applications*, CRC press, 2017.
18- Xu, Y. ed. Two-Dimensional Nanostructures for Energy-Related Applications, 2016.
19- Greco, Ralph S., Fritz B. Prinz, and R. Lane Smith, eds. *Nanoscale technology in biological systems*. CRC press, 2004.
20- Wilson, Mick, et al. "Nanotechnology: basic science and emerging technologies." (2002).

21- Pearson, G. S. *Perchlorates: A review of their thermal decomposition and combustion, with an appendix on perchloric acid*. RPE, 1968.

22- Nye, Rachel Anna. "Nucleation and Growth Mechanisms in Atomic and Molecular Layer Deposition for Applications in Microelectronics and Metal-Organic Frameworks." (2022).
23- Whitesides, George M., John P. Mathias, and Christopher T. Seto. "Molecular self-assembly and nanochemistry: a chemical strategy for the synthesis of nanostructures." *Science* 254.5036 (1991): 1312-1319.

24- Fuchs, Peter, Yaroslav E. Romanyuk, and Ayodhya N. Tiwari. "Chemical Bath Deposition." *Transparent Conductive Materials: Materials, Synthesis, Characterization, Applications* (2018): 81-103.

25- Nadimpalli, Nagaravi Kumar Varma, Rajdip Bandyopadhyaya, and Venkataramana Runkana. "Thermodynamic analysis of hydrothermal synthesis of nanoparticles." *Fluid Phase Equilibria* 456 (2018): 33-45.

26- Mahan, John E. *Physical vapor deposition of thin films*. 2000.

27- Stolle, Achim, and Brindaban Ranu, eds. *Ball milling towards green synthesis: applications, projects, challenges*. Royal Society of Chemistry, 2014.

28- Gyorgy, E., et al. "Bioactive glass and hydroxyapatite thin films obtained by pulsed laser deposition." *Applied surface science* 253.19 (2007): 7981-7986.

29- Stringfellow, Gerald B. *Organometallic vapor-phase epitaxy: theory and practice*. Elsevier, 1999.

30- Kim, Myungjoon, et al. "Synthesis of nanoparticles by laser ablation: A review." *KONA Powder and Particle Journal* 34 (2017): 80-90.

31- Semaltianos, N. G. "Nanoparticles by laser ablation." *Critical reviews in solid state and materials sciences* 35.2 (2010): 105-124.

32- Sylvestre, J-P., et al. "Femtosecond laser ablation of gold in water: influence of the laser-produced plasma on the nanoparticle size distribution." *Applied Physics A* 80 (2005): 753-758.

33- Tsuji, Takeshi, et al. "Preparation of silver nanoparticles by laser ablation in solution: influence of laser wavelength on particle size." *Applied surface science* 202.1-2 (2002): 80-85.

34- Zeng, Haibo, et al. "Nanomaterials via laser ablation/irradiation in liquid: a review." *Advanced Functional Materials* 22.7 (2012): 1333-1353.

35- Ahmed, Shakeel, and Saiqa Ikram, eds. *Chitosan: derivatives, composites and applications*. John Wiley & Sons, 2017.

36- Lee, K. H. "Chitosan as a Biomaterial—Structure, Properties, and Electrospun Nanofibers". Concepts in Tissue Engineering, chapter 6,2021.

37- Rinaudo, Marguerite. "Chitin and chitosan: Properties and applications." *Progress in polymer science* 31.7 (2006): 603-632.

38- Chandra, S., Chakraborty, N., Dasgupta, A., Sarkar, J., Panda, K., & Acharya, K. (2015). Chitosan nanoparticles: a positive modulator of innate immune responses in plants. *Scientific reports*, *5*(1), 15195..

39- Fang, Zhongxiang, et al. "Active and intelligent packaging in meat industry." *Trends in Food Science & Technology* 61 (2017): 60-71.

40- Marin, Luminita, Bogdan Simionescu, and Mihail Barboiu. "Imino-chitosan biodynamers." *Chemical Communications* 48.70 (2012): 8778-8780.

41- Mucha, Maria, Joanna Piekielna, and Anna Wieczorek. "Characterisation and morphology of biodegradable chitosan/synthetic polymer blends." *Macromolecular symposia*. Vol. 144. No. 1. Weinheim, Germany: WILEY-VCH Verlag GmbH & Co. KGaA, 1999.

42- Mucha, Maria, Joanna Piekielna, and Anna Wieczorek. "Characterisation and morphology of biodegradable chitosan/synthetic polymer blends." *Macromolecular symposia*. Vol. 144. No. 1. Weinheim, Germany: WILEY-VCH Verlag GmbH & Co. KGaA, 1999.

43- Crini, Grégorio. "Recent developments in polysaccharide-based materials used as adsorbents in wastewater treatment." *Progress in polymer science* 30.1 (2005): 38-70.

44- Vakili, Mohammadtaghi, et al. "Application of chitosan and its derivatives as adsorbents for dye removal from water and wastewater: A review." *Carbohydrate polymers* 113 (2014): 115-130.

45- Li, Peng, et al. "A polycationic antimicrobial and biocompatible hydrogel with microbe membrane suctioning ability." *Nature materials* 10.2 (2011): 149-156.

46- Dharma, Hadi Nugraha Cipta, et al. "A review of titanium dioxide (TiO2)-based photocatalyst for oilfield-produced water treatment." *Membranes* 12.3 (2022): 345.

47- Luttrell, Tim, et al. "Why is anatase a better photocatalyst than rutile?-Model studies on epitaxial TiO2 films." *Scientific reports* 4.1 (2014): 4043.

48- Jiang, Jing, et al. "Synthesis and facet-dependent photoreactivity of BiOCl single-crystalline nanosheets." *Journal of the American Chemical Society* 134.10 (2012): 4473-4476.

49- Fu, Guifen, Patricia S. Vary, and Chhiu-Tsu Lin. "Anatase TiO2 nanocomposites for antimicrobial coatings." *The journal of physical chemistry B* 109.18 (2005): 8889-8898.

50- Cho, Min, et al. "Linear correlation between inactivation of E. coli and OH radical concentration in TiO2 photocatalytic disinfection." *Water research* 38.4 (2004): 1069-1077.

51- Fujishima, Akira, Tata N. Rao, and Donald A. Tryk. "Titanium dioxide photocatalysis." *Journal of photochemistry and photobiology C: Photochemistry reviews* 1.1 (2000): 1-21.

52- Greenwood, Norman Neill, and Alan Earnshaw. *Chemistry of the Elements*. Elsevier, 2012.

53- Nowotny, Janusz. *Oxide semiconductors for solar energy conversion: titanium dioxide*. CRC press, 2011.

54- He, Xue-Long, et al. "Room temperature cold sprayed TiO2 scattering layer for high performance and bending resistant plastic-based dye-sensitized solar cells." *Journal of Power Sources* 251 (2014): 122-129.

55- Rai, Mahendra, Alka Yadav, and Aniket Gade. "Silver nanoparticles as a new generation of antimicrobials." *Biotechnology advances* 27.1 (2009): 76-83.

56- Ashcroft, N. W., and N. D. Mermin. "Solid State Physics, Holt, Rinehart and Winston." *New York* 2005 (1976): 403.

57- Parveen, Suphiya, Ranjita Misra, and Sanjeeb K. Sahoo. "Nanoparticles: a boon to drug delivery, therapeutics, diagnostics and imaging." *Nanomedicine in cancer* (2017): 47-98.

58- Huh, Ae Jung, and Young Jik Kwon. "“Nanoantibiotics”: a new paradigm for treating infectious diseases using nanomaterials in the antibiotics resistant era." *Journal of controlled release* 156.2 (2011): 128-145.

59- Durak, Rıdvan, and Yüksel Özdemır. "Measurement of K-shell fluorescence cross-sections and yields of 14 elements in the atomic number range 25⩽ Z⩽ 47 using photoionization." *Radiation Physics and Chemistry* 61.1 (2001): 19-25.

60- Atasoy, Evren, and Nizamettin Kahraman. "Diffusion bonding of commercially pure titanium to low carbon steel using a silver interlayer." *Materials characterization* 59.10 (2008): 1481-1490.

61- Rathjen, Andreas, et al. "Adhesion and Electrical Properties of Low Temperature Processed Ag-PMMA-Films in Inkjet Printing." *NIP & Digital Fabrication Conference*. Vol. 31. Society for Imaging Science and Technology, 2015.

62- Martynková, Gražyna Simha, et al. "Effect of Milling and Annealing on Carbon–Silver System." *Journal of nanoscience and nanotechnology* 19.5 (2019): 2770-2774.

63- Amendola, Vincenzo, Stefano Polizzi, and Moreno Meneghetti. "Laser ablation synthesis of silver nanoparticles embedded in graphitic carbon matrix." *Science of Advanced Materials* 4.3-4 (2012): 497-500.

64- Nielsen, Brent L., and Lyle R. Brown. "The basis for colored silver-protein complex formation in stained polyacrylamide gels." *Analytical biochemistry* 141.2 (1984): 311-315.

65- Hebb, Malcolm H. "Electrical conductivity of silver sulfide." *The journal of chemical physics* 20.1 (1952): 185-190.

66- Zhu, Yalin, et al. "Novel metal coated nanoencapsulated phase change materials with high thermal conductivity for thermal energy storage." *Solar energy materials and solar cells* 176 (2018): 212-221.

67- Gutierrez, P. Carolina, et al. "Color and golden shine of silver Islamic luster." *Journal of the American Ceramic Society* 93.8 (2010): 2320-2328.

68- PAULY, HANS. "Hardness of cryolite, chiolite, cryolithionite and other fluorides from Ivigtut, South Greenland." *B. Geol. Soc. Denmark* 34 (1985): 145-150.

69- Lobodin, Vladislav V., et al. "Separation and characterization of reactive and non-reactive sulfur in petroleum and its fractions." *Energy & Fuels* 29.10 (2015): 6177-6186.

70- Natsuki, Jun, Toshiaki Natsuki, and Yoshio Hashimoto. "A review of silver nanoparticles: synthesis methods, properties and applications." *Int. J. Mater. Sci. Appl* 4.5 (2015): 325-332.

71- Rai, Mahendra, Alka Yadav, and Aniket Gade. "Silver nanoparticles as a new generation of antimicrobials." *Biotechnology advances* 27.1 (2009): 76-83.

72- Foster, Howard A., et al. "Photocatalytic disinfection using titanium dioxide: spectrum and mechanism of antimicrobial activity." *Applied microbiology and biotechnology* 90 (2011): 1847-1868.

73- Brown, Ashley N., et al. "Nanoparticles functionalized with ampicillin destroy multiple-antibiotic-resistant isolates of Pseudomonas aeruginosa and Enterobacter aerogenes and methicillin-resistant Staphylococcus aureus." *Applied and environmental microbiology* 78.8 (2012): 2768-2774.

74- Kang, Seoktae, et al. "Single-walled carbon nanotubes exhibit strong antimicrobial activity." *Langmuir* 23.17 (2007): 8670-8673.

75- Raghupathi, Krishna R., Ranjit T. Koodali, and Adhar C. Manna. "Size-dependent bacterial growth inhibition and mechanism of antibacterial activity of zinc oxide nanoparticles." *Langmuir* 27.7 (2011): 4020-4028.

76- Todar, Kenneth. "Textbook of bacteriology." (2015).

77- Madigan, Michael T., John M. Martinko, and Jack Parker. *Brock biology of microorganisms*. Vol. 11. Upper Saddle River, NJ: Prentice hall, 1997.

78- Alberts, Bruce. *Molecular biology of the cell*. Garland science, 2017.

79- Examples of bacterial species, no specific reference.

80- Ryan, Kenneth James, C. George Ray, and John C. Sherris. "Sherris medical microbiology: an introduction to infectious diseases." *(No Title)* (2004).

81- Gerritsen, Jacoline, et al. "Intestinal microbiota in human health and disease: the impact of probiotics." *Genes & nutrition* 6 (2011): 209-240.

82- Croxen, Matthew A., et al. "Recent advances in understanding enteric pathogenic Escherichia coli." *Clinical microbiology reviews* 26.4 (2013): 822-880.

83- Madigan, Michael T., John M. Martinko, and Jack Parker. *Brock biology of microorganisms*. Vol. 11. Upper Saddle River, NJ: Prentice hall, 1997.

84- Ryan, K. J. Sherris medical microbiology: an introduction to infectious diseases. McGraw-Hill Medical Publishing, 1994.

85- Gyles, C. L., and J. M. Fairbrother. "Escherichia coli." *Pathogenesis of bacterial infections in animals* 4 (2010): 267-308.

86- Martin, Rebekah M., and Michael A. Bachman. "Colonization, infection, and the accessory genome of Klebsiella pneumoniae." *Frontiers in cellular and infection microbiology* 8 (2018): 4.

87- Nordmann, Patrice, and Laurent Poirel. "The difficult-to-control spread of carbapenemase producers among Enterobacteriaceae worldwide." *Clinical Microbiology and Infection* 20.9 (2014): 821-830.

88- Imlay, James A. "Pathways of oxidative damage." *Annual Reviews in Microbiology* 57.1 (2003): 395-418.

89- Janeway, Charles, et al. *Immunobiology: the immune system in health and disease*. Vol. 2. New York: Garland Pub., 2001.

90- Clokie, Martha RJ, et al. "Phages in nature." *Bacteriophage* 1.1 (2011): 31-45.

91- Feng, Qing Ling, et al. "A mechanistic study of the antibacterial effect of silver ions on Escherichia coli and Staphylococcus aureus." *Journal of biomedical materials research* 52.4 (2000): 662-668.

92- Ventola, C. Lee. "The antibiotic resistance crisis: part 1: causes and threats." *Pharmacy and therapeutics* 40.4 (2015): 277.

93- Haldorai, Yuvaraj, and Jae-Jin Shim. "Novel chitosan-TiO2 nanohybrid: Preparation, characterization, antibacterial, and photocatalytic properties." *Polymer Composites* 35.2 (2014): 327-333.

94- A Salman, Amenah. "Synthesis and Characterization of TiO2 Nanoparticles by Laser Ablation in Liquid." *Engineering and Technology Journal* 34.1 (2016): 100-106.

95- Raut, A. V., et al. "Synthesis and characterization of chitosan-TiO2: Cu nanocomposite and their enhanced antimicrobial activity with visible light." *Colloids and Surfaces B: Biointerfaces* 148 (2016): 566-575.

96- Regiel-Futyra, Anna, et al. "Development of noncytotoxic silver–chitosan nanocomposites for efficient control of biofilm forming microbes." *RSC advances* 7.83 (2017): 52398-52413.

97- Jbeli, A., et al. "Chitosan-Ag-TiO2 films: an effective photocatalyst under visible light." *Carbohydrate polymers* 199 (2018): 31-40.

98- Menazea, A. A., and Nasser S. Awwad. "Antibacterial activity of TiO2 doped ZnO composite synthesized via laser ablation route for antimicrobial application." *Journal of Materials Research and Technology* 9.4 (2020): 9434-9441.

99- Menazea, A. A., and Nasser S. Awwad. "Antibacterial activity of TiO2 doped ZnO composite synthesized via laser ablation route for antimicrobial application." *Journal of Materials Research and Technology* 9.4 (2020): 9434-9441.

100- Khashan, Khawla S., et al. "Antibacterial activity of TiO2 nanoparticles prepared by one-step laser ablation in liquid." *Applied Sciences* 11.10 (2021): 4623.

101- Martínez-Chávez, Luis Alejandro, et al. "Au-Ag/TiO2 Thin Films Preparation by Laser Ablation and Sputtering Plasmas for Its Potential Use as Photoanodes in Electrochemical Advanced Oxidation Processes (EAOP)." *Catalysts* 11.11 (2021): 1406.

102- Kadhum, Mohammed A., Tahseen H. Mubarak, and Nadia M. Jassim. "Structural and Fluorescence Properties of TiO2/Ag Nanoparticles Bilayers." *Diyala Journal For Pure Science* 17.03 (2021).

103- Iordanova, E., et al. "Ultra-short laser pulse modification of chitosan/silver nanoparticles (AgNPs) thin films for potential antimicrobial applications." *IOP Conference Series: Materials Science and Engineering*. Vol. 1056. No. 1. IOP Publishing, 2021..

104- Rafiq, Aftab, et al. "Biosynthesis of silver nanoparticles from novel Bischofia javanica plant loaded chitosan hydrogel: as antimicrobial and wound healing agent." *Biomass Conversion and Biorefinery* (2022): 1-11.

105- Alheshibri, Muidh, et al. "Synthesis of Ag nanoparticles-decorated on CNTs/TiO2 nanocomposite as efficient photocatalysts via nanosecond pulsed laser ablation." *Optics & Laser Technology* 155 (2022): 108443.

106- Ali, Heba, A. M. Ismail, and A. A. Menazea. "Multifunctional Ag/ZnO/chitosan ternary bio-nanocomposites synthesized via laser ablation with enhanced optical, antibacterial, and catalytic characteristics." *Journal of Water Process Engineering* 49 (2022): 102940.

107- BARIĆ, Gordana. "Charles P. Poole Jr. i Frank J. Owens: Introduction to Nanotechnology." *Polimeri: časopis za plastiku i gumu* 24.2-4 (2003): 134-135.

108- Barnes, Bill. "Optical Properties of Solids, 2nd edn, by Mark Fox: Scope: monograph. Level: undergraduate, postgraduate, early career researcher, researcher." (2011): 612-613.

109- Smith, F. Graham, Terry A. King, and Dan Wilkins. *Optics and photonics: an introduction*. John Wiley & Sons, 2007.

110- Ibraheim, Adil M., and Maki A. Sameer. "Effect of The Cu Doping on The Structural and Optical Properties of AlSb Thin Films Deposited by Thermal Evaporation Method." *Journal of Physics: Conference Series*. Vol. 1879. No. 3. IOP Publishing, 2021.

111- Wang, Xuewan, et al. "Quantum dots derived from two-dimensional materials and their applications for catalysis and energy." *Chemical Society Reviews* 45.8 (2016): 2239-2262.

112- Ibach, Harald, and Hans Lüth. *Solid-state physics: an introduction to principles of materials science*. Springer Science & Business Media, 2009.

113- Wehrenberg, Brian L., Congjun Wang, and Philippe Guyot-Sionnest. "Interband and intraband optical studies of PbSe colloidal quantum dots." *The Journal of Physical Chemistry B* 106.41 (2002): 10634-10640.

114- Tauc, J. Amorphous and Liquid Semiconductors. Springer US, 1974.

115- Mott, Nevill Francis, and Edward A. Davis. *Electronic processes in non-crystalline materials*. Oxford university press, 2012.

116- Smith, Brian C. *Fundamentals of Fourier transform infrared spectroscopy*. CRC press, 2011.

117- Vyvyan, James R., et al. "Preparing students for research: Synthesis of substituted chalcones as a comprehensive guided-inquiry experience." *Journal of chemical education* 79.9 (2002): 1119.

118- Stuart, Barbara H. *Infrared spectroscopy: fundamentals and applications*. John Wiley & Sons, 2004.

119- Goldstein, Joseph I., et al. *Scanning electron microscopy and X-ray microanalysis*. springer, 2017.

120- Egerton, Ray F. *Physical principles of electron microscopy*. Vol. 56. New York: Springer, 2005.

121- Goldstein, Joseph I., et al. *Scanning electron microscopy and X-ray microanalysis*. springer, 2017.

122- Reed, Stephen Jervis Brent. *Electron microprobe analysis and scanning electron microscopy in geology*. Cambridge university press, 2005.

123- Cullity, B. D., and S. R. Stock. "Elements of x-ray diffraction, Prentice Hall." *Upper Saddle River, NJ* (2001): 388.

124- Kluh, H. P., and L. E. Alexander. "X-ray Diffraction Procedures for Polycrystalline and Amorphous Materials." *Wiley, New York 1974* (1974).

125- Langford, J. I. "X-ray diffraction procedures for polycrystalline and amorphous materials by HP Klug and LE Alexander." *Journal of Applied Crystallography* 8.5 (1975): 573-574.

126- Pecharsky, Vitalij K., and Peter Y. Zavalij. *Fundamentals of diffraction*. Springer US, 2003.

127- Kaku, Tomomi, et al. "Proteomic analysis of the G-layer in poplar tension wood." *Journal of Wood Science* 55.4 (2009): 250-257.

128- Goldstein, Joseph I., et al. *Scanning electron microscopy and X-ray microanalysis*. springer, 2017.

129- Egerton, Ray F. *Physical principles of electron microscopy*. Vol. 56. New York: Springer, 2005.

130- Carter, David B. Williams C. Barry. *Transmission Electron Microscopy A Textbook for Materials Science*. springer publication, 2009.

131- Zhang, Dongmao, et al. "Chemical segregation and reduction of Raman background interference using drop coating deposition." *Applied spectroscopy* 58.8 (2004): 929-933.

132- Winterowd, Jack G., and Paul A. Sandford. "Chitin and chitosan." *FOOD SCIENCE AND TECHNOLOGY-NEW YORK-MARCEL DEKKER-* (1995): 441-441.

133- Pang, Tianting, et al. "Removal of fluoride from water using activated carbon fibres modified with zirconium by a drop-coating method." *Chemosphere* 255 (2020): 126950.

134- Carter, David B. Williams C. Barry. *Transmission Electron Microscopy A Textbook for Materials Science*. springer publication, 2009.

135- WA, RUTALA. "Guideline for disinfection and sterilization in healthcare facilities." *http://www. cdc. gov/hicpac/pdf/guidelines/Disinfection_Nov_2008. pdf. Accessed 2008* (2008).

136- BinSabt, Mohammad, et al. "Green synthesis of CS-TiO2 NPs for efficient photocatalytic degradation of methylene blue dye." *Polymers* 14.13 (2022): 2677.

137- Tajdidzadeh, M., et al. "Synthesis of silver nanoparticles dispersed in various aqueous media using laser ablation." *The Scientific World Journal* 2014 (2014).

138- Sionkowska, Alina. "Effects of solar radiation on collagen and chitosan films." *Journal of Photochemistry and Photobiology B: Biology* 82.1 (2006): 9-15.

139- Xu, Peng, et al. "Magnetic separable chitosan microcapsules decorated with silver nanoparticles for catalytic reduction of 4-nitrophenol." *Journal of colloid and interface science* 507 (2017): 353-359.

140- Ashkarran, A. A. "Antibacterial properties of silver-doped TiO2 nanoparticles under solar simulated light." (2011): 1-8.

141- Pastoriza-Santos, Isabel, et al. "One-pot synthesis of Ag@ TiO2 core− shell nanoparticles and their layer-by-layer assembly." *Langmuir* 16.6 (2000): 2731-2735.

142- Skoog, Douglas A., et al. *Fundamentals of analytical chemistry*. Cengage learning, 2013.

143- Foot, Christopher J. *Atomic physics*. Vol. 7. OUP Oxford, 2004.

144- Samuels, Robert Joel. "Solid state characterization of the structure of chitosan films." *Journal of polymer science: polymer physics edition* 19.7 (1981): 1081-1105.

145- Gong, Sai, and Bang-Gui Liu. "Electronic structures and optical properties of TiO2: Improved density-functional-theory investigation." *Chinese Physics B* 21.5 (2012): 057104.

146- Jian-Zhi, Zhao, Wang Guang-Tao, and Liang Yong-Cheng. "Mechanical properties and electronic structures of cotunnite TiO2." *Chinese Physics Letters* 25.12 (2008): 4356.

147- Bhosale, J., et al. "Temperature dependence of band gaps in semiconductors: Electron-phonon interaction." *Physical Review B* 86.19 (2012): 195208.

148- Zhang, Hua, and Steven H. Neau. "In vitro degradation of chitosan by a commercial enzyme preparation: effect of molecular weight and degree of deacetylation." *Biomaterials* 22.12 (2001): 1653-1658.

149- Zeng, Jie, et al. "Controlling the shapes of silver nanocrystals with different capping agents." *Journal of the American Chemical Society* 132.25 (2010): 8552-8553.

150- Huang, Xiaofei, et al. "A novel silver-loaded chitosan composite sponge with sustained silver release as a long-lasting antimicrobial dressing." *RSC advances* 7.55 (2017): 34655-34663.